Precision measurements of Higgs boson properties with the ATLAS experiment

Martina Javurkova

(University of Massachusetts-Amherst)

On behalf of the ATLAS collaboration

Cracow Epiphany Conference 2024

8th - 12th January 2024

Introduction

- Higgs boson is a **fundamental particle**, even under CP inversion, predicted by the BEH mechanism
- **Higgs boson mass** is not predicted by the theory and needs to be estimated experimentally
  - Stability of the electroweak vacuum (i.e. of our universe) depends on this value
- **Strength of the interaction** between the Higgs boson and other elementary particles
  - Predicted by the SM once the Higgs boson mass is known
  - **Gauge couplings**: essential test of the spontaneous electroweak symmetry breaking
  - **Yukawa couplings**: important test of the CP structure of the Higgs boson couplings
- The best possible knowledge of its properties is essential
  - Test the SM
  - Any deviation could imply new physics
    - Parametrised within the ***κ*-** or **EFT framework**

Piled Higher and Deeper (PHD Comics)

More than 10 years since its discovery

- **Run 1**: Higgs boson discovery announced by ATLAS and CMS in 2012 (~10 ifb @7/8 TeV)
- **Full Run 2 dataset**: 30 times more Higgs events than at the time of its discovery (139 ifb @13 TeV)
- **Run 3 ongoing**: hopefully the statistics will triple (so far ~66 ifb @13.6 TeV)

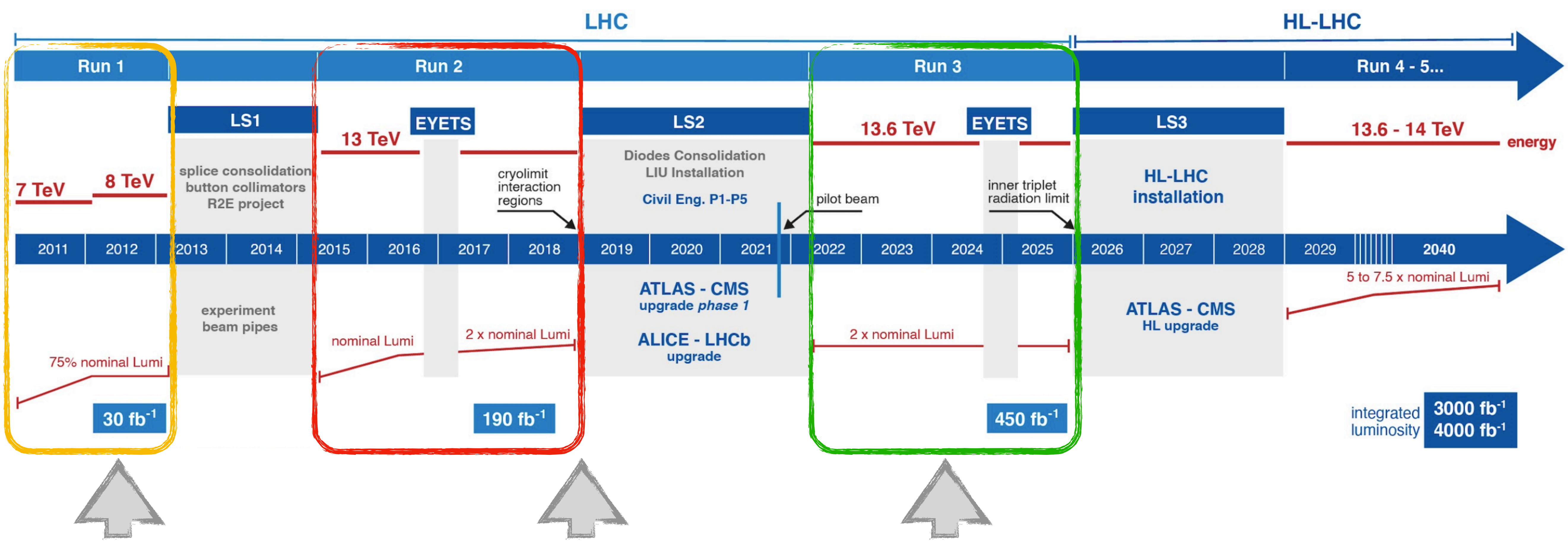

Higgs boson discovery   Most results presented use full Run 2 data   Today   LHC/HL-LHC plan

ATLAS CMS

More than 10 years since its discovery

- **Run 1**: Higgs boson discovery announced by ATLAS and CMS in 2012 (~10 ifb @7/8 TeV)
- **Full Run 2 dataset**: 30 times more Higgs events than at the time of its discovery (139 ifb @13 TeV)
- **Run 3 ongoing**: hopefully the statistics will triple (so far ~66 ifb @13.6 TeV)

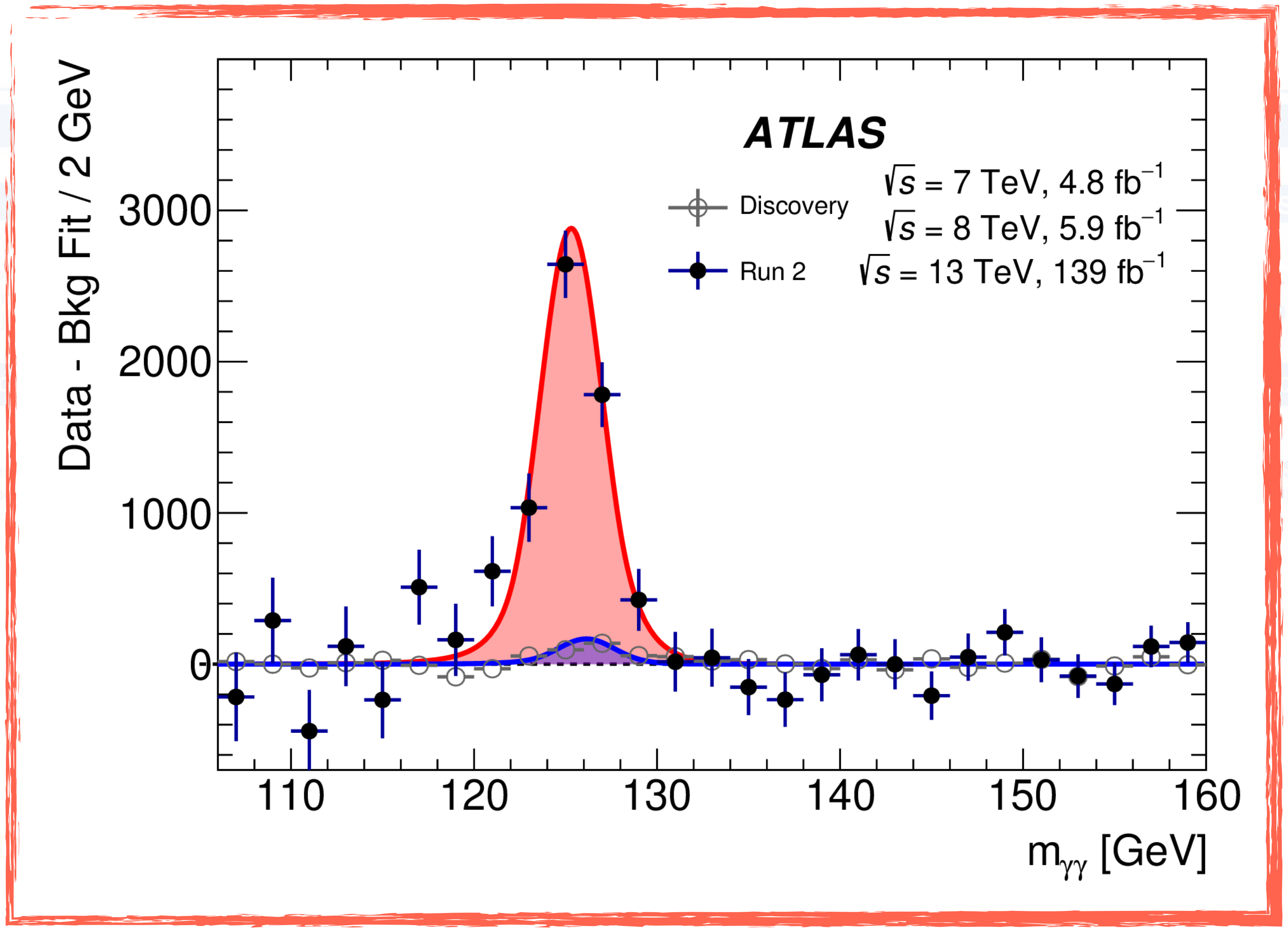

[Nature 607, 52 (2022)]

Higgs boson production

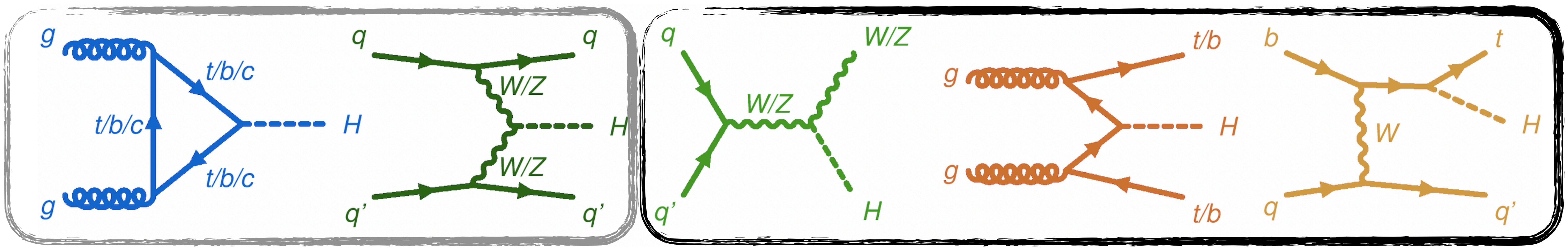

- About 9M Higgs bosons produced in ATLAS (~27k reconstructed) during Run 2
- **ggF** is the dominant production process at LHC and provides <u>indirect</u> measurement of *top Yukawa coupling* via virtual loops
- **ttH** provides <u>direct</u> measurement of *top Yukawa coupling*
- **ggF** and **VBF** observed during **<u>Run 1</u>**
- **WH**, **ZH** and **ttH+tH** observed during **<u>Run 2</u>**

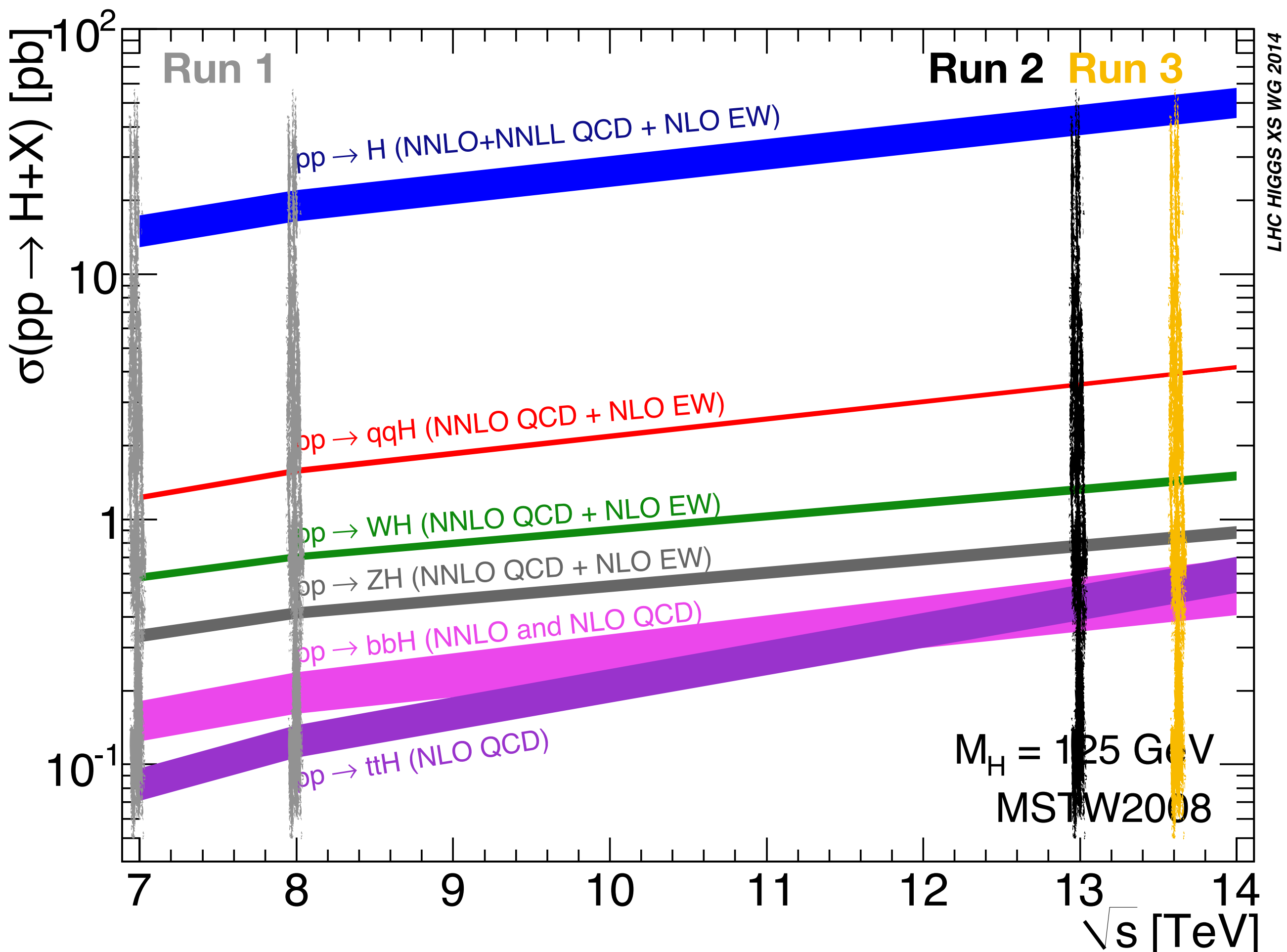

LHC Higgs WG twiki

Higgs boson production

Nature 607, 52 (2022)

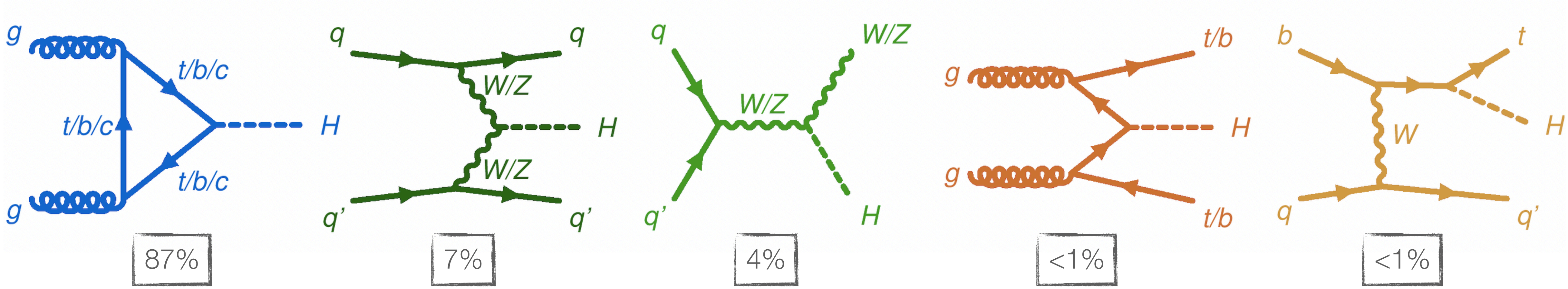

- About 9M Higgs bosons produced in ATLAS (~27k reconstructed) during Run 2
- **ggF** is the dominant production process at LHC and provides <u>indirect</u> measurement of *top Yukawa coupling* via virtual loops
- **ttH** provides <u>direct</u> measurement of *top Yukawa coupling*
- **ggF** and **VBF** observed during **<u>Run 1</u>**
- **WH**, **ZH** and **ttH+tH** observed during **<u>Run 2</u>**

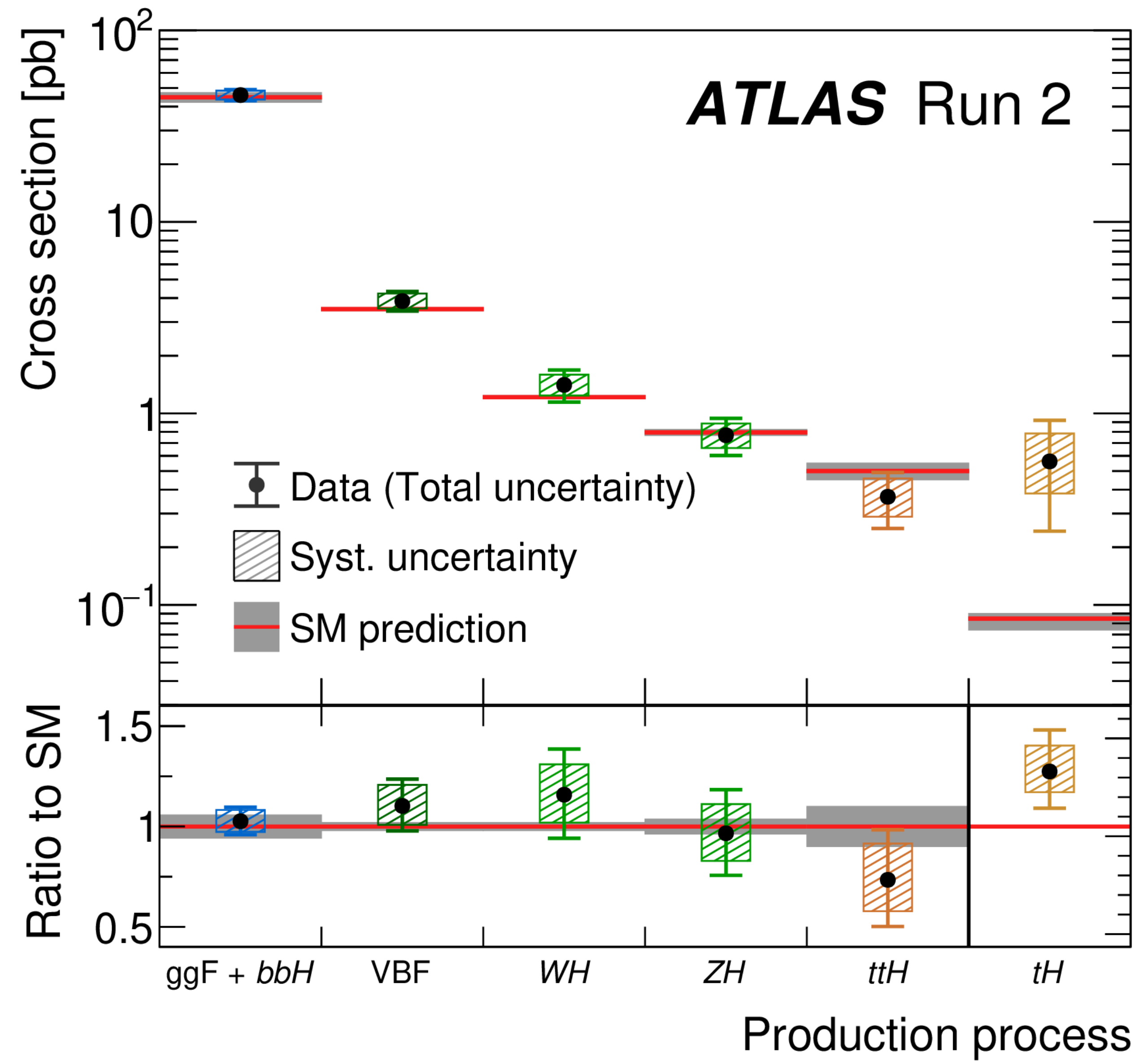

Higgs boson decay

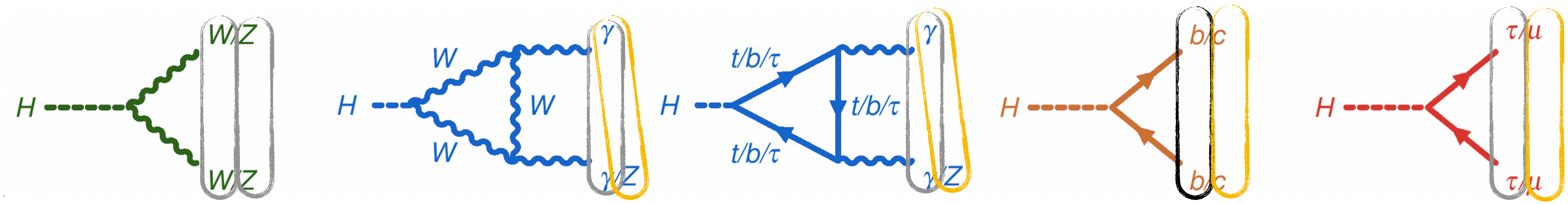

- First discovered in bosonic decay channels: $H \to ZZ^*$, $H \to WW^*$, $H \to \gamma\gamma$
- Interactions with third generation fermions well measured: $H \to \tau\tau$, $H \to b\bar{b}$
- Measurements of Higgs couplings to second-generation fermions challenging: $H \to \mu\mu$, $H \to c\bar{c}$
- $\gamma\gamma$, **ZZ**, **WW** and $\tau\tau$ observed during **Run 1**
- $\mathbf{b\bar{b}}$ observed during **Run 2** / $\mu\mu$, $Z\gamma$, $c\bar{c}$ not yet

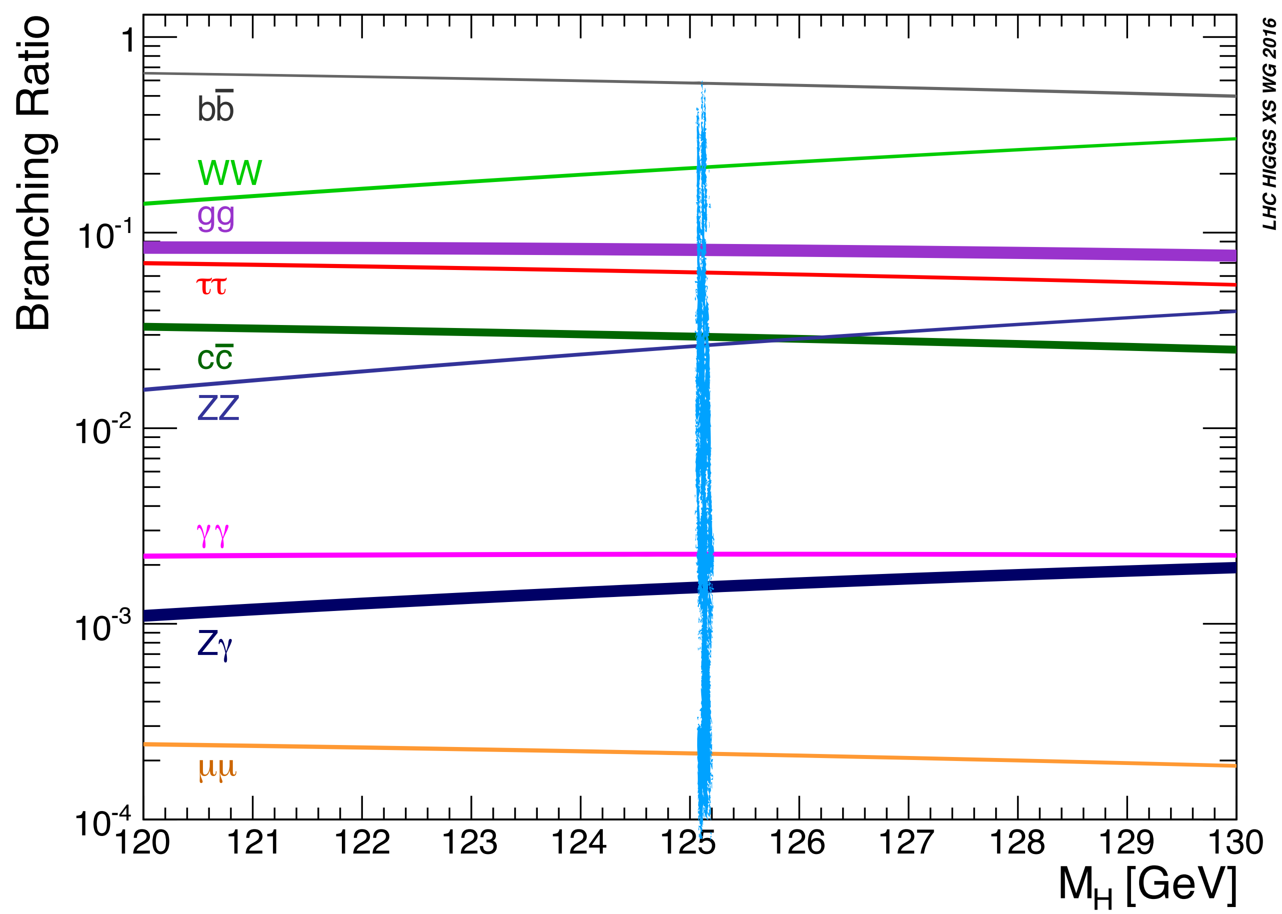

Higgs boson decay

[Nature 607, 52 (2022)]

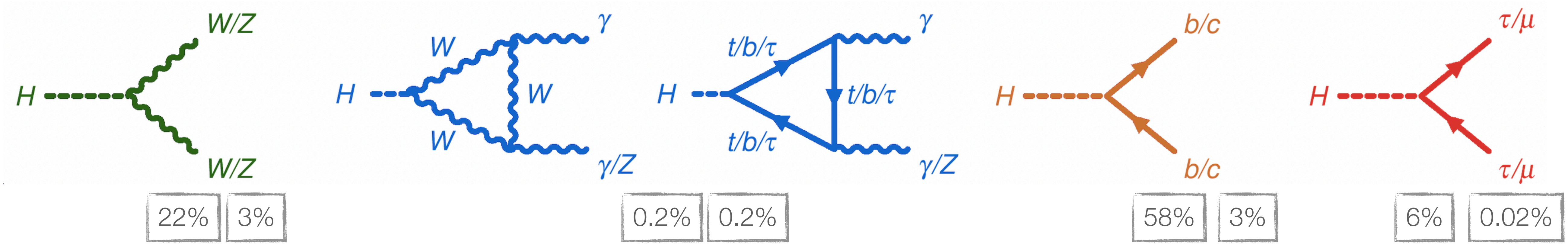

- First discovered in bosonic decay channels: $H \to ZZ^*$, $H \to WW^*$, $H \to \gamma\gamma$
- Interactions with third generation fermions well measured: $H \to \tau\tau$, $H \to b\bar{b}$
- Measurements of Higgs couplings to second-generation fermions challenging: $H \to \mu\mu$, $H \to c\bar{c}$
- $\gamma\gamma$, **ZZ**, **WW** and $\tau\tau$ observed during **Run 1**
- $\mathbf{b\bar{b}}$ observed during **Run 2** / $\mu\mu$, $Z\gamma$, $c\bar{c}$ not yet

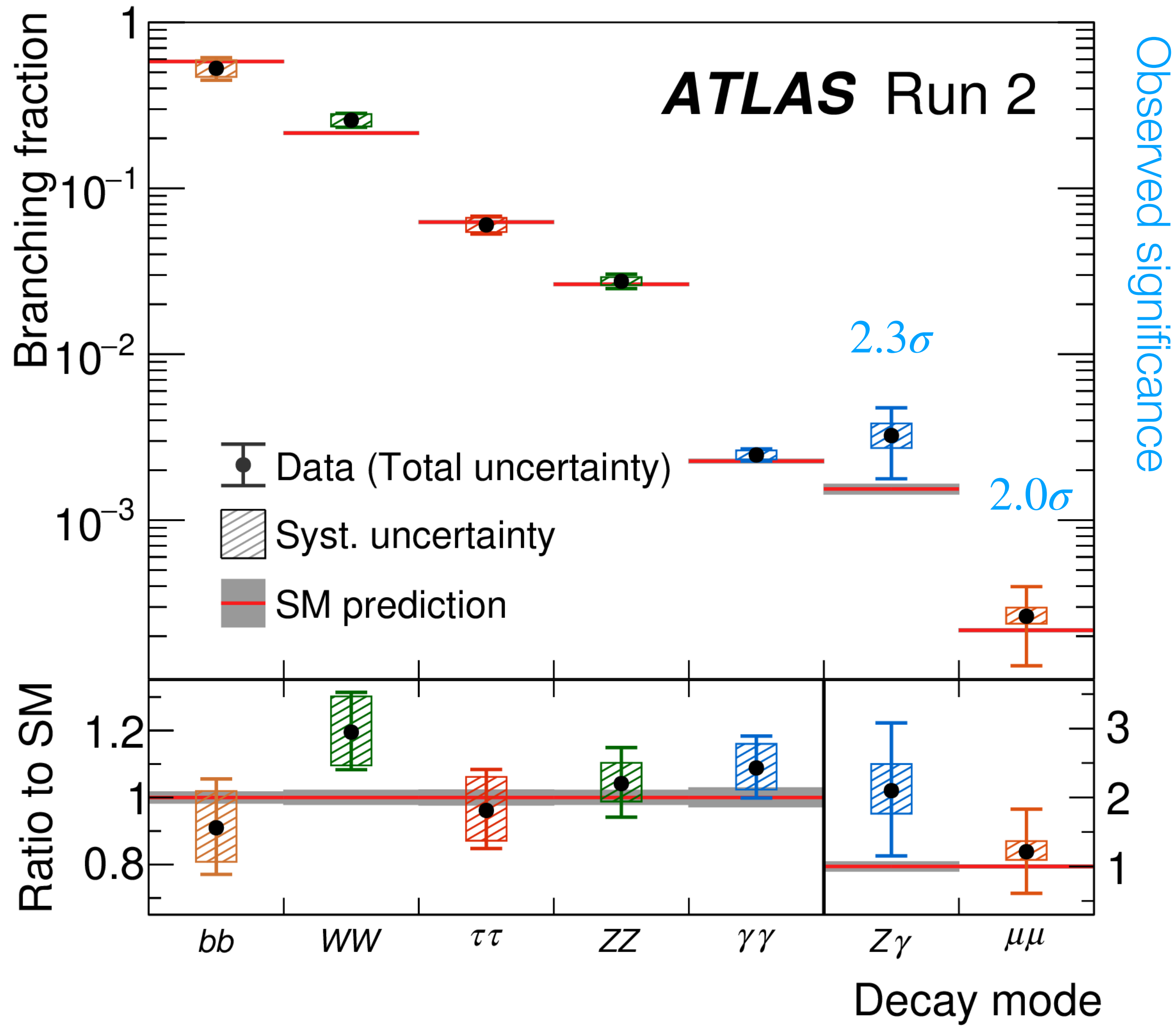

Higgs boson production and decay
Nature 607, 52 (2022)

- Different combinations of Higgs production and decay ($\sigma \times B$) measurements allow detailed tests of the SM
  - Excellent agreement with the SM prediction (**p-value=72%**)
- Combined measurement of the inclusive Higgs production cross-section
  - Assuming that all production and decay processes scale with the **same** global signal strength[1]
  - $\mu = 1.05 \pm 0.03\,(\text{stat.}) \pm 0.03\,(\text{exp.}) \pm 0.04\,(\text{sig.th.}) \pm 0.02\,(\text{bkg.th.}) = 1.05 \pm 0.06$

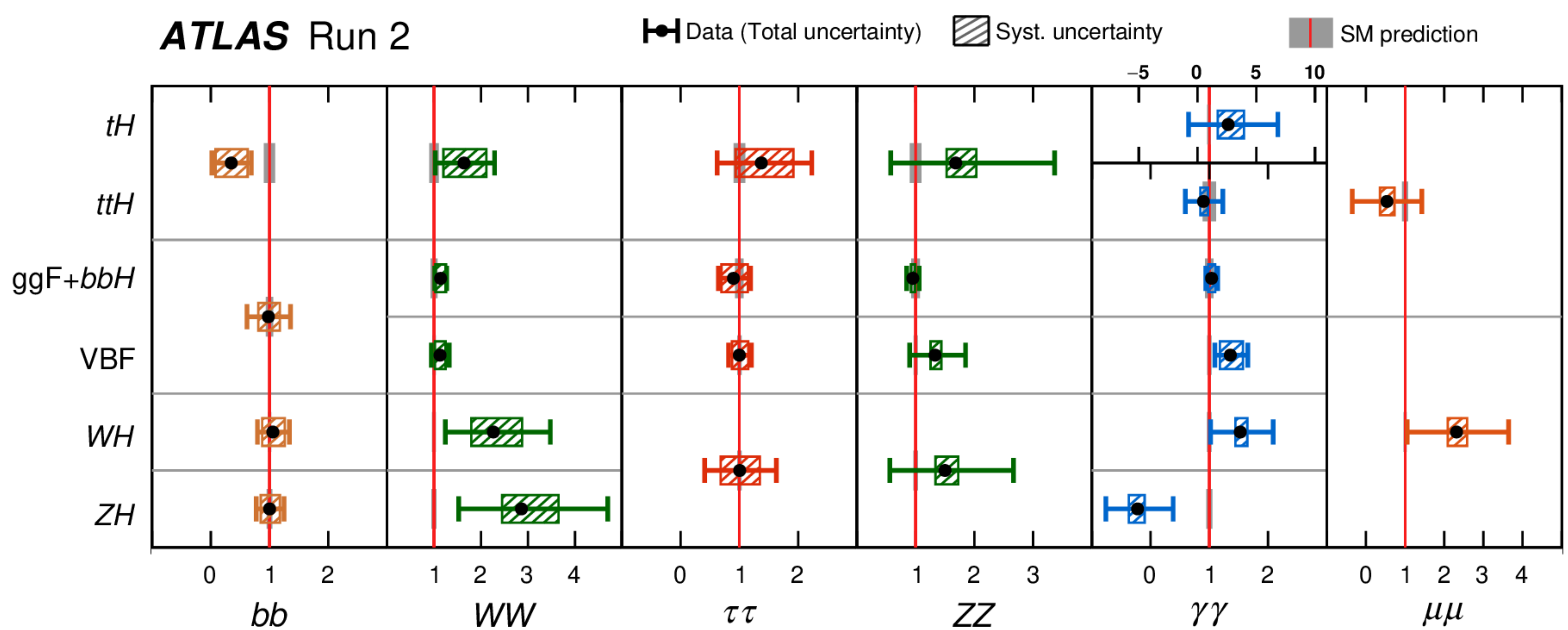

[1] $\mu = \mu_{if} = (\sigma_i/\sigma_i^{SM}) \times (B_f/B_f^{SM})$

Higgs boson couplings

Nature 607, 52 (2022)

- Results interpreted within the **κ-framework** with a set of **coupling strength modifiers**[1]: $\kappa_p^2 = \sigma_p/\sigma_p^{SM}$ or $\kappa_p^2 = \Gamma_p/\Gamma_p^{SM}$
  - Scaling of the Higgs couplings to the SM particles as a function of their mass agrees with the SM
  - Most of the κ-modifiers measured with an accuracy of 5%-12%

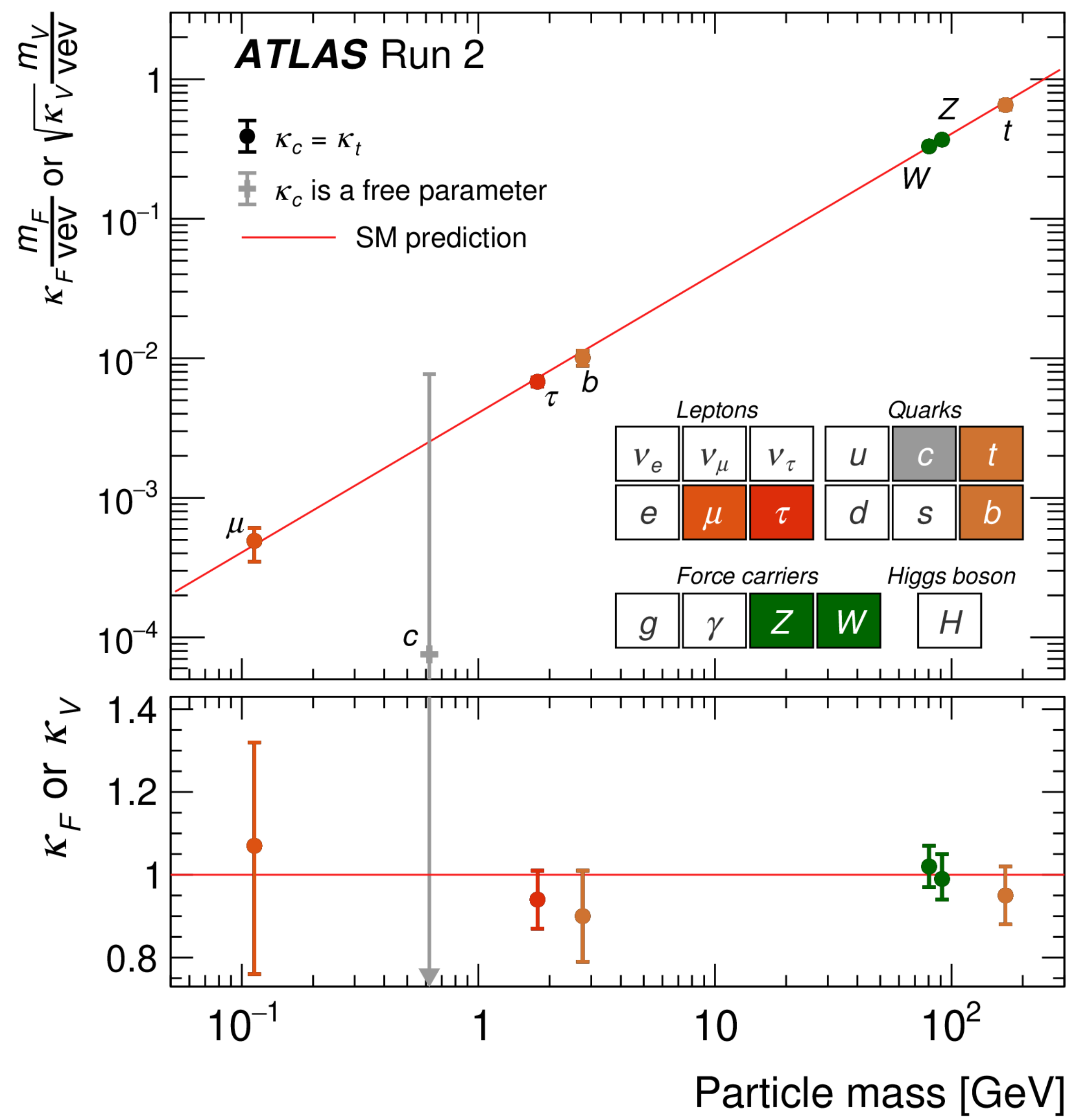

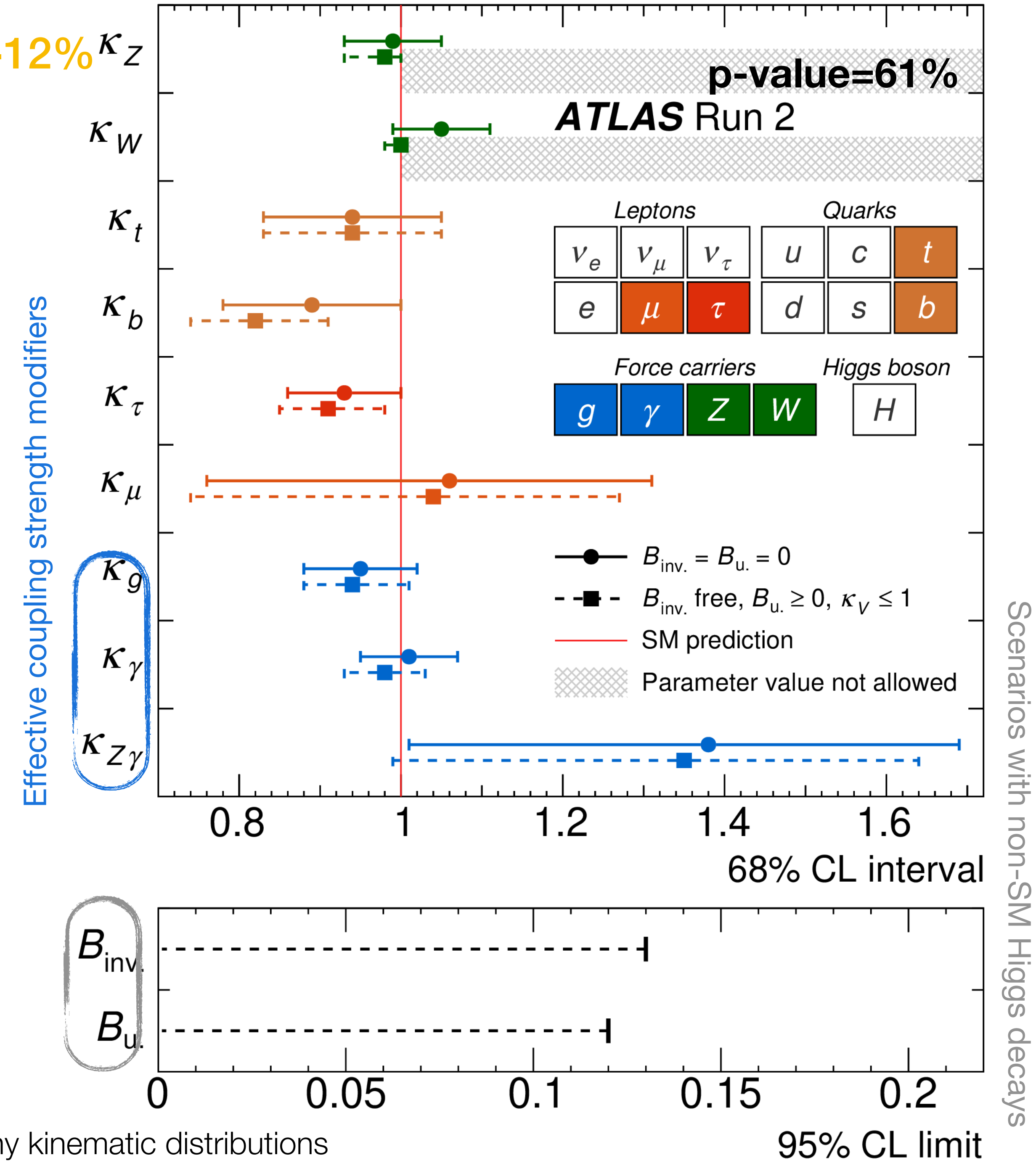

[1] Assuming that BSM physics modifies only the Higgs coupling strengths without altering any kinematic distributions

Simplified template x-sections

- **STXS** = powerful framework for Higgs cross-section production measurements
  - Enables studying **kinematic properties** of the Higgs production and probing the internal structure of its couplings
  - Partitions phase space into **mutually exclusive regions** specific to different Higgs production modes
  - Allows for a combination of all measurements in different decay channels
  - Maximises experimental sensitivity
  - Minimising the dependence on theoretical uncertainties that are directly folded into the measurements

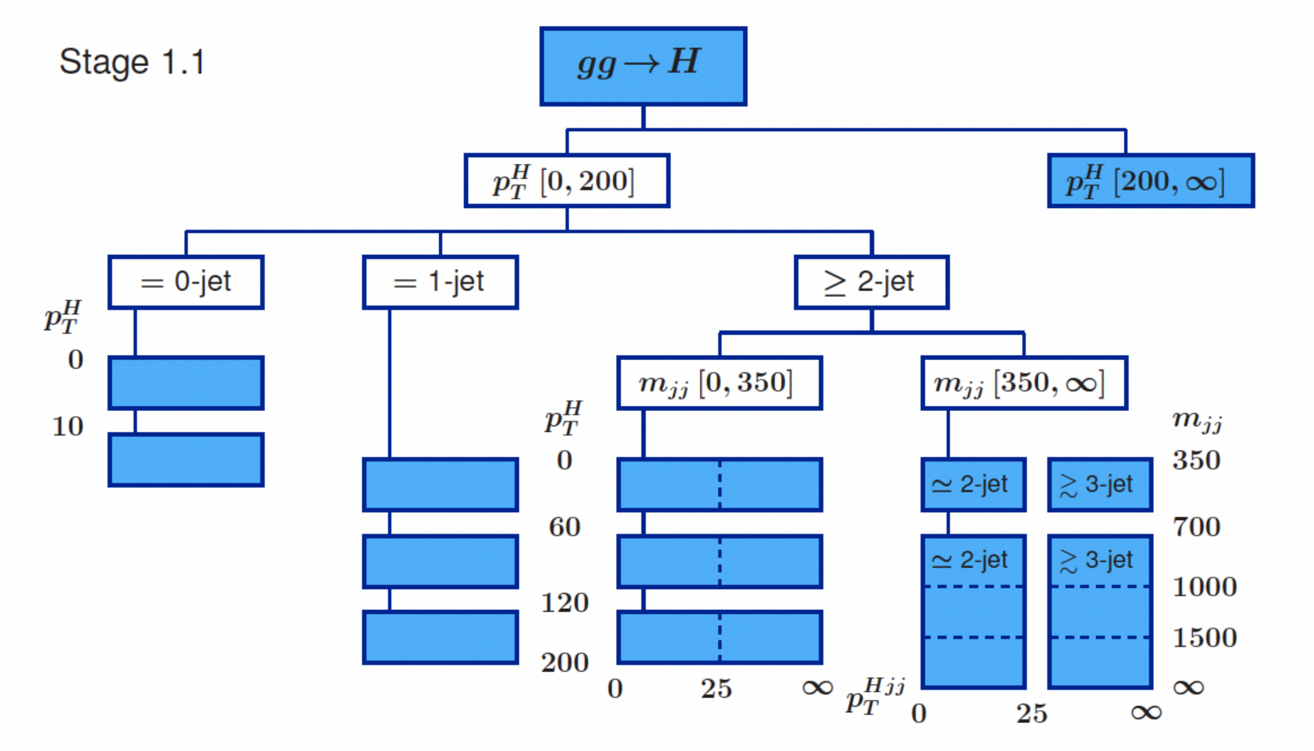

Simplified Template Cross Sections - Stage 1.1

Simplified template x-sections

Nature 607, 52 (2022)

- **Full Run 2 results** performed in 36 regions consistent with the SM predictions (**p-value=94%**)

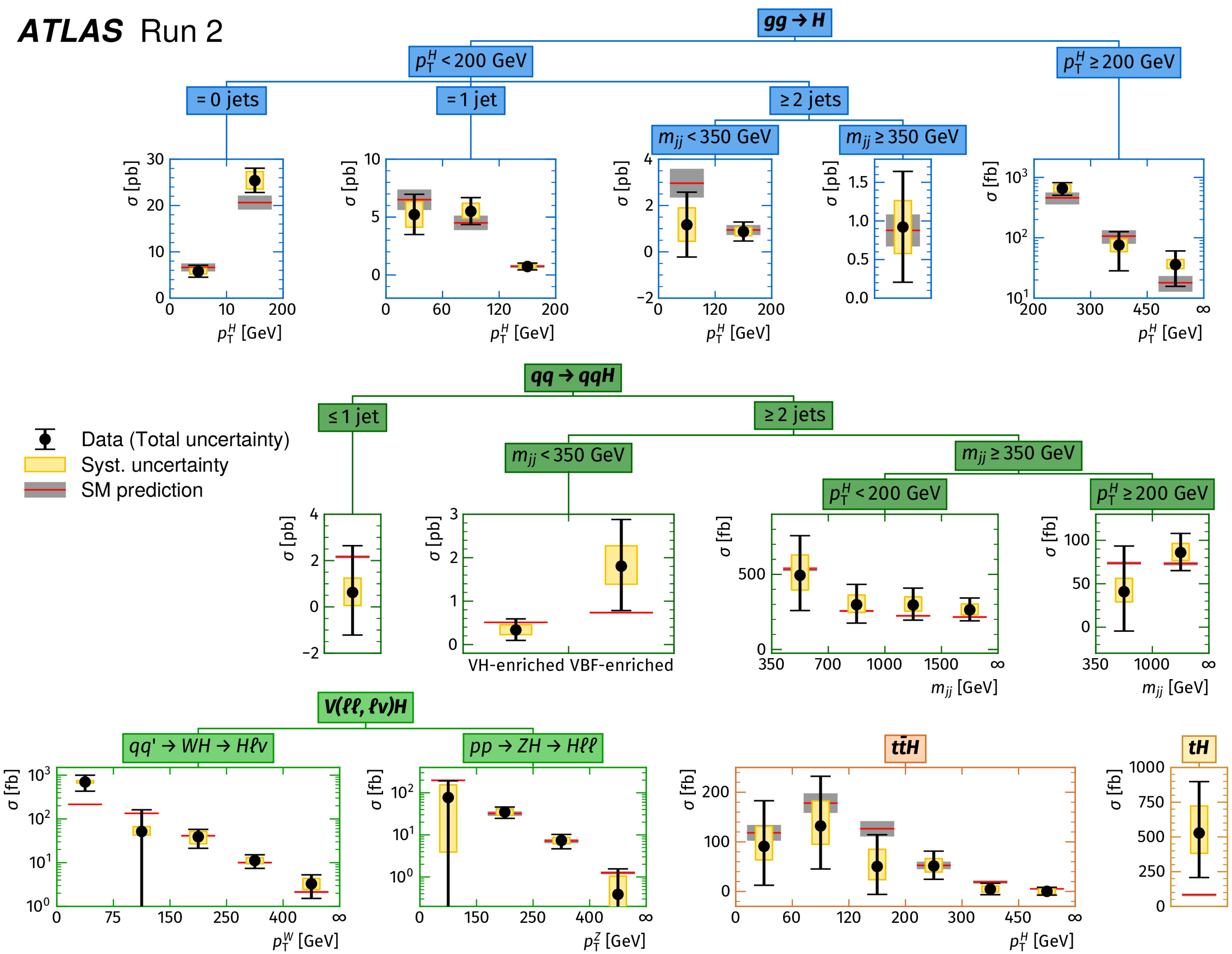

Explored **high p_T^H regime** where sensitivity to new physics is expected to be enhanced.

Fiducial x-sections

- **Fiducial x-section** = x-section measured in a phase space closely matching **detector** and **analysis** acceptance
  - Minimises extrapolation effects (extrapolation to the full phase space often required to combine analyses)
  - Enough data to perform not only inclusive but also **differential** x-section measurements
    - Measurements performed *as a function of various variables* sensitive to the properties of Higgs boson
  - Measured cross-sections corrected for detector inefficiency and resolution to the particle level, through **unfolding**

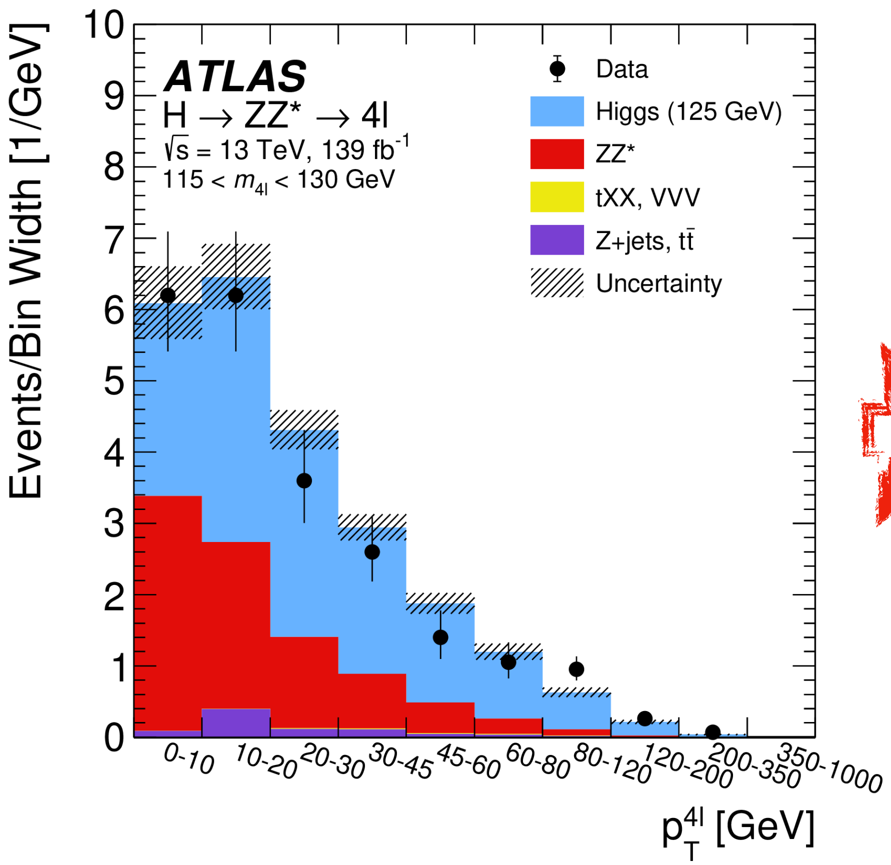

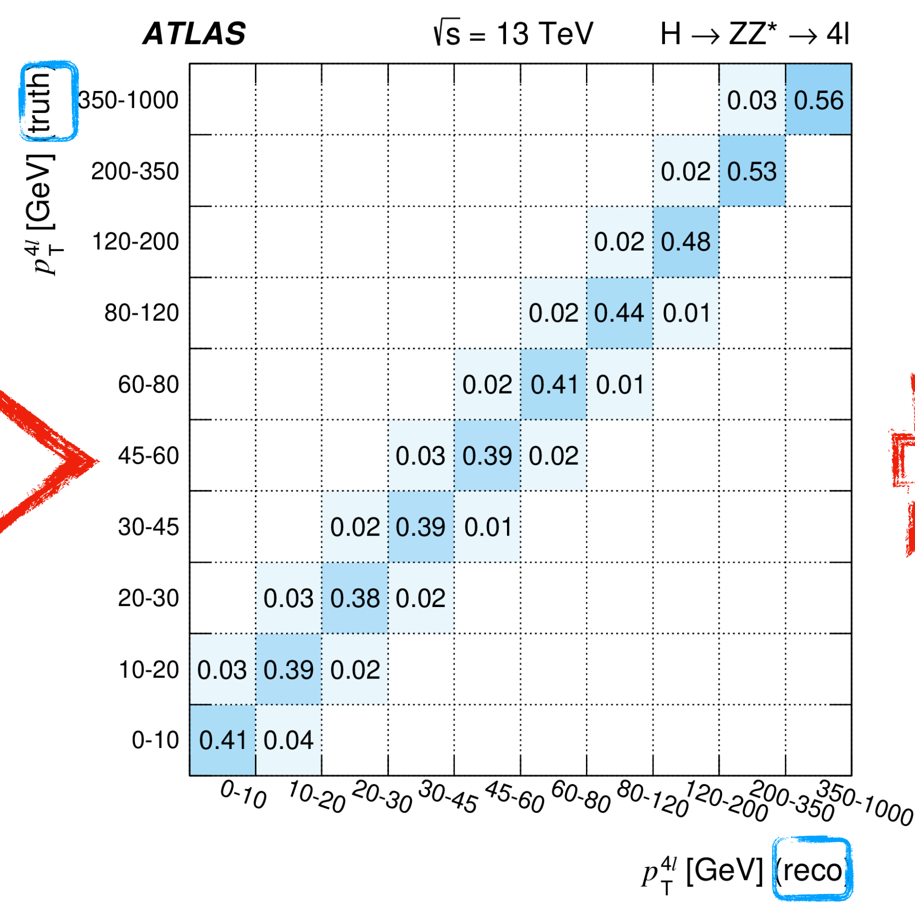

Detector response matrix

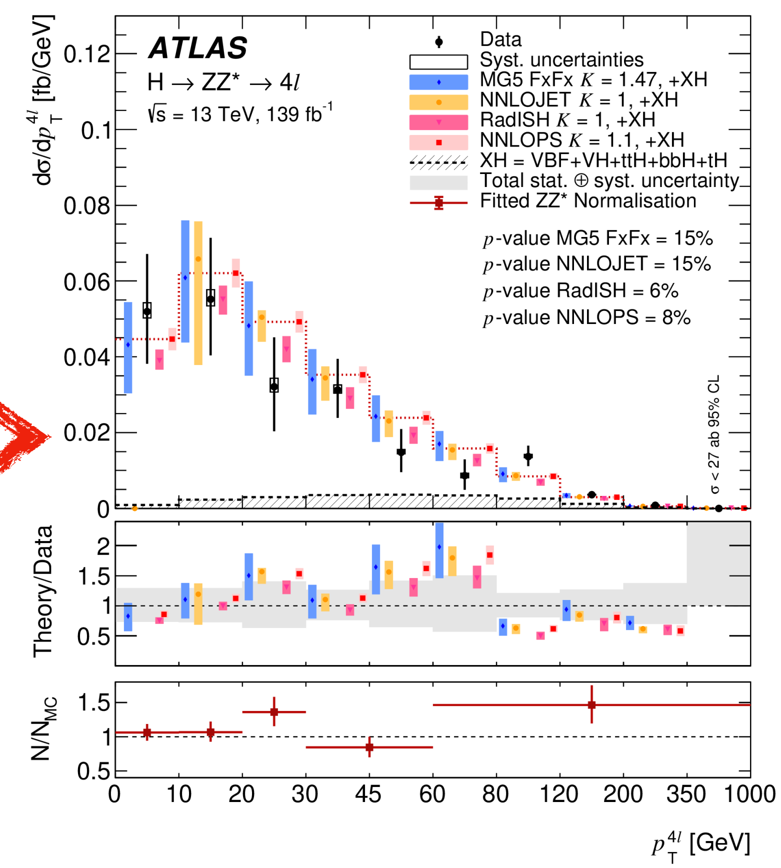

EPJC 80 (2020) 942

x-sections in ggF $H \to WW^* \to e\nu\mu\nu$ EPJC 83 (2023) 774

- Single- and double-differential measurements performed in **ggF-enriched region** ($N_{\rm jet} < 2$)
- Signal in each interval of the observable under consideration is extracted from a **fit to m_T**
- **8 observables** sensitive to the Higgs production ($p_{\rm T}^H$, $|y_{j0}|$) and decay ($p_{\rm T}^{\ell 0}$, $p_T^{\ell\ell}$, $m_{\ell\ell}$, $y_{\ell\ell}$, $\Delta\phi_{\ell\ell}$, $\cos\theta^*$) kinematics
- Normalisations of WW, top-quark and Z/γ^* bkgs obtained from the simultaneous fit to data using dedicated CRs
- Dominant **systematic uncertainties**: jet and muon reconstruction, theoretical modelling of top and WW bkgs

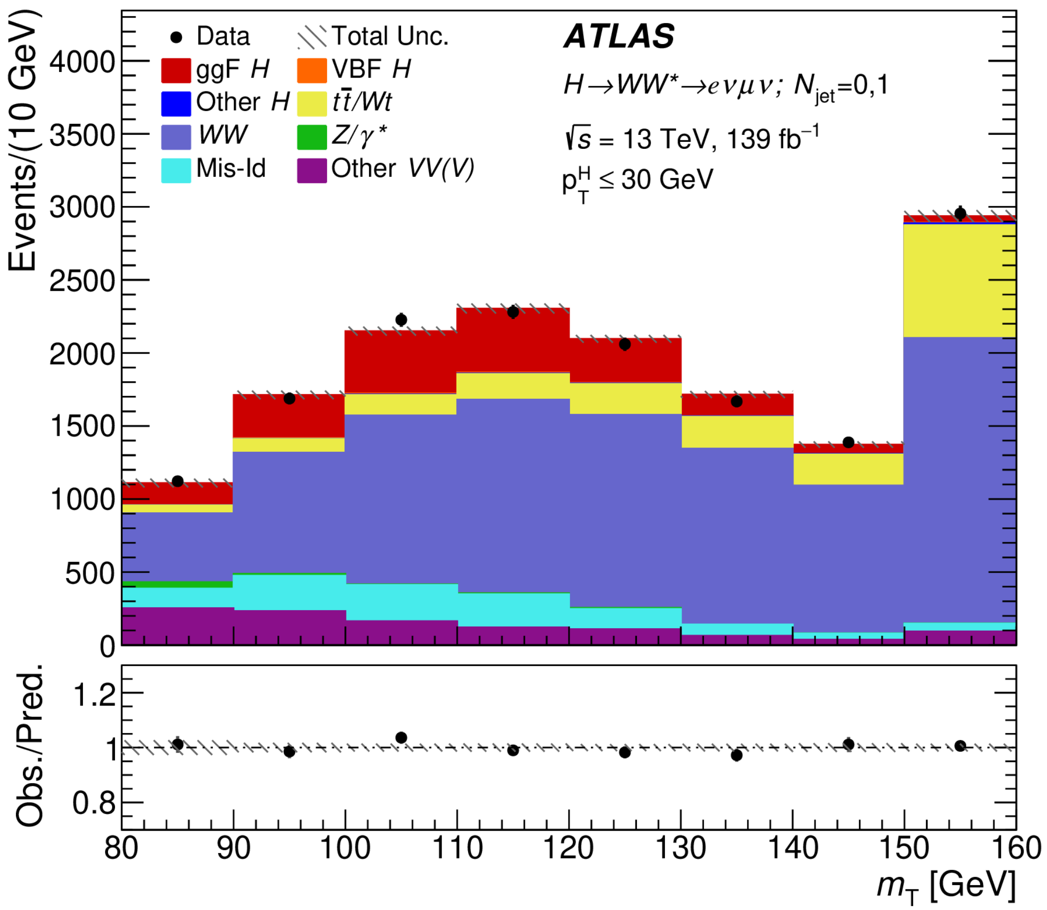

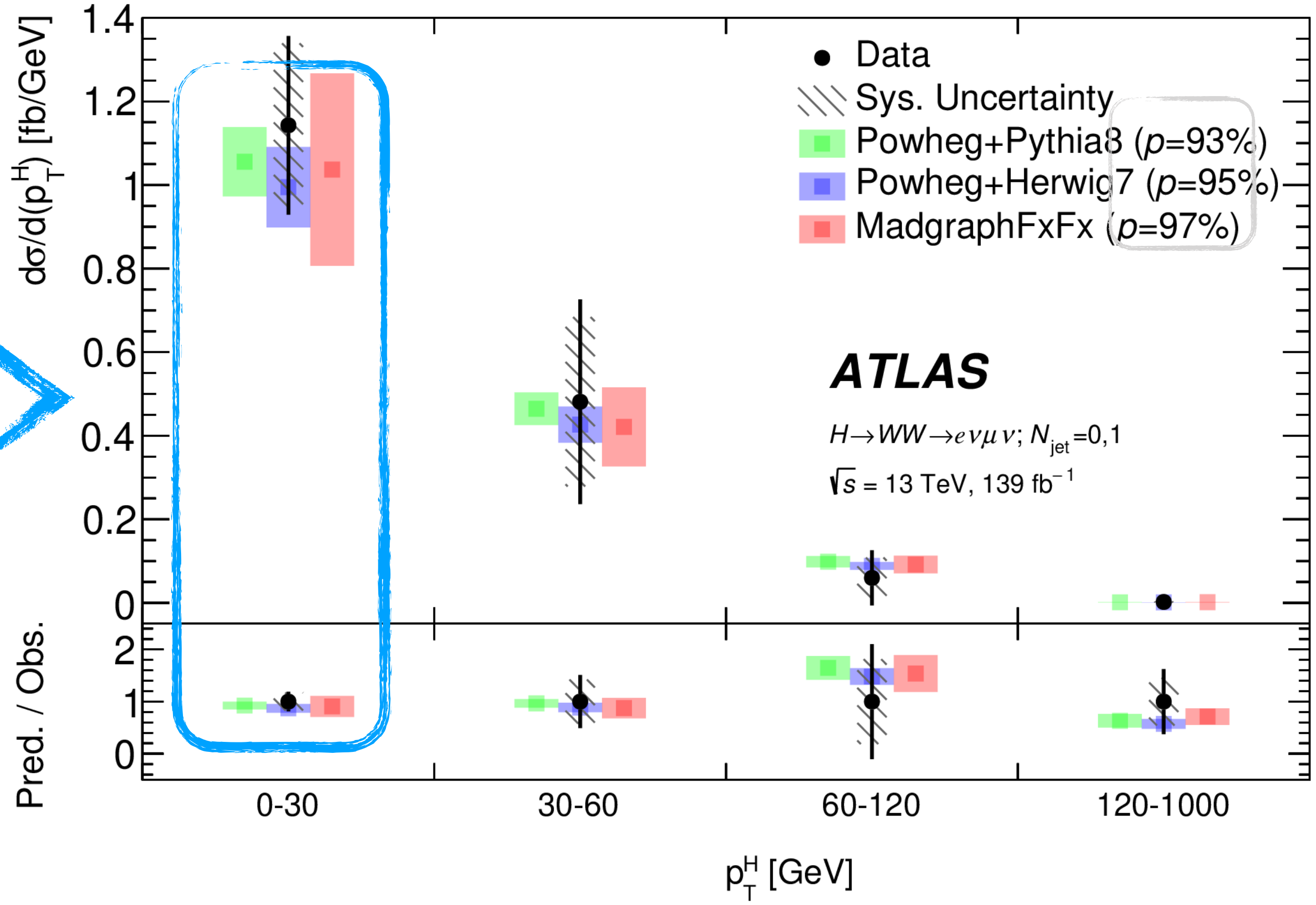

Very good agreement with the SM

x-sections in VBF $H \to WW^* \to e\nu\mu\nu$ PRD 108, 072003

- Integrated x-section measurements performed in **VBF-enriched region** ($N_{\mathrm{jet}} \geq 2$)
- Dedicated BDT discriminants used to separate VBF from top+VV and top+VV from other backgrounds
- Overall relative precision is about 23%, dominated by the **statistical uncertainty** in the data sample
  - Dominant systematic uncertainties are theoretical (signal modelling), largest experimental uncertainty is JER
  - $\sigma^{\mathrm{fid}} = 1.68 \pm 0.33(\mathrm{stat.}) \pm 0.23(\mathrm{syst.})\,\mathrm{fb} = 1.68 \pm 0.40\,\mathrm{fb}$

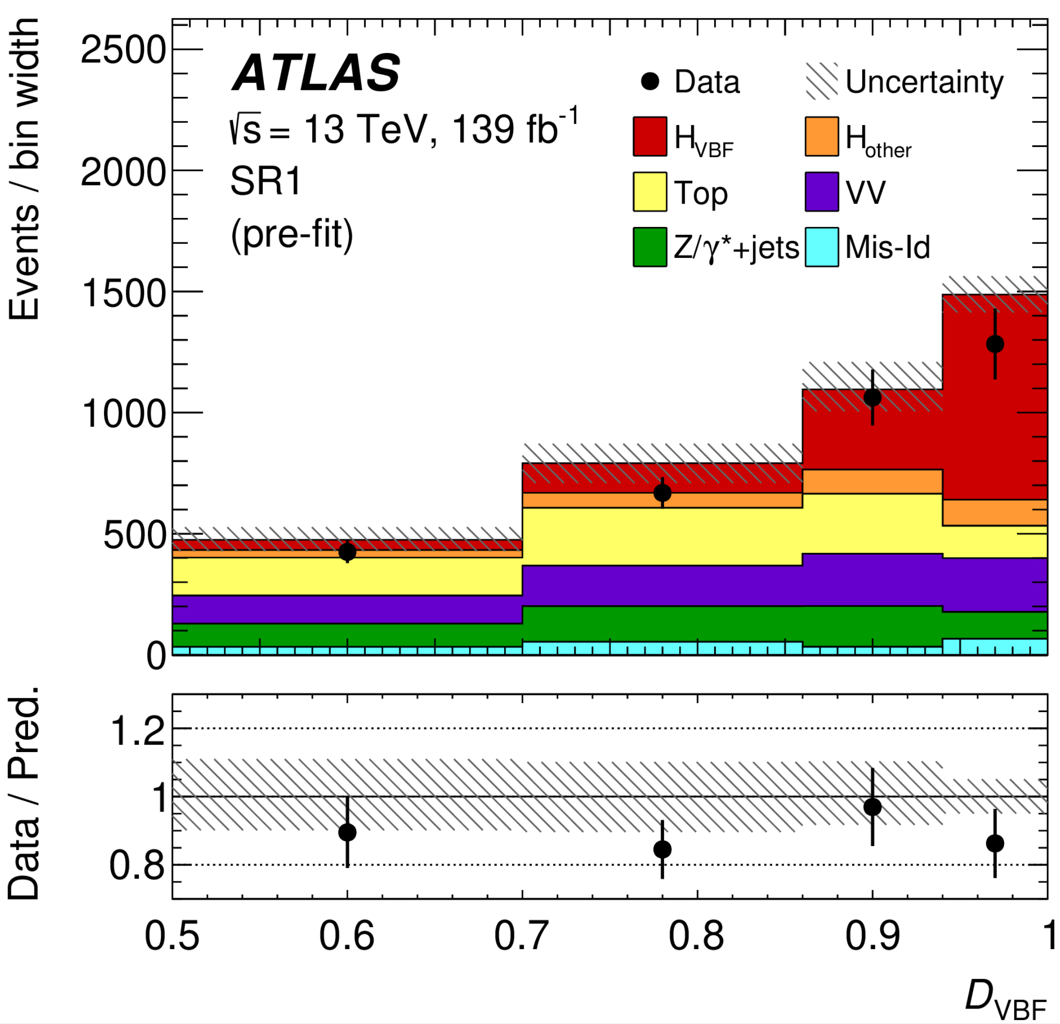

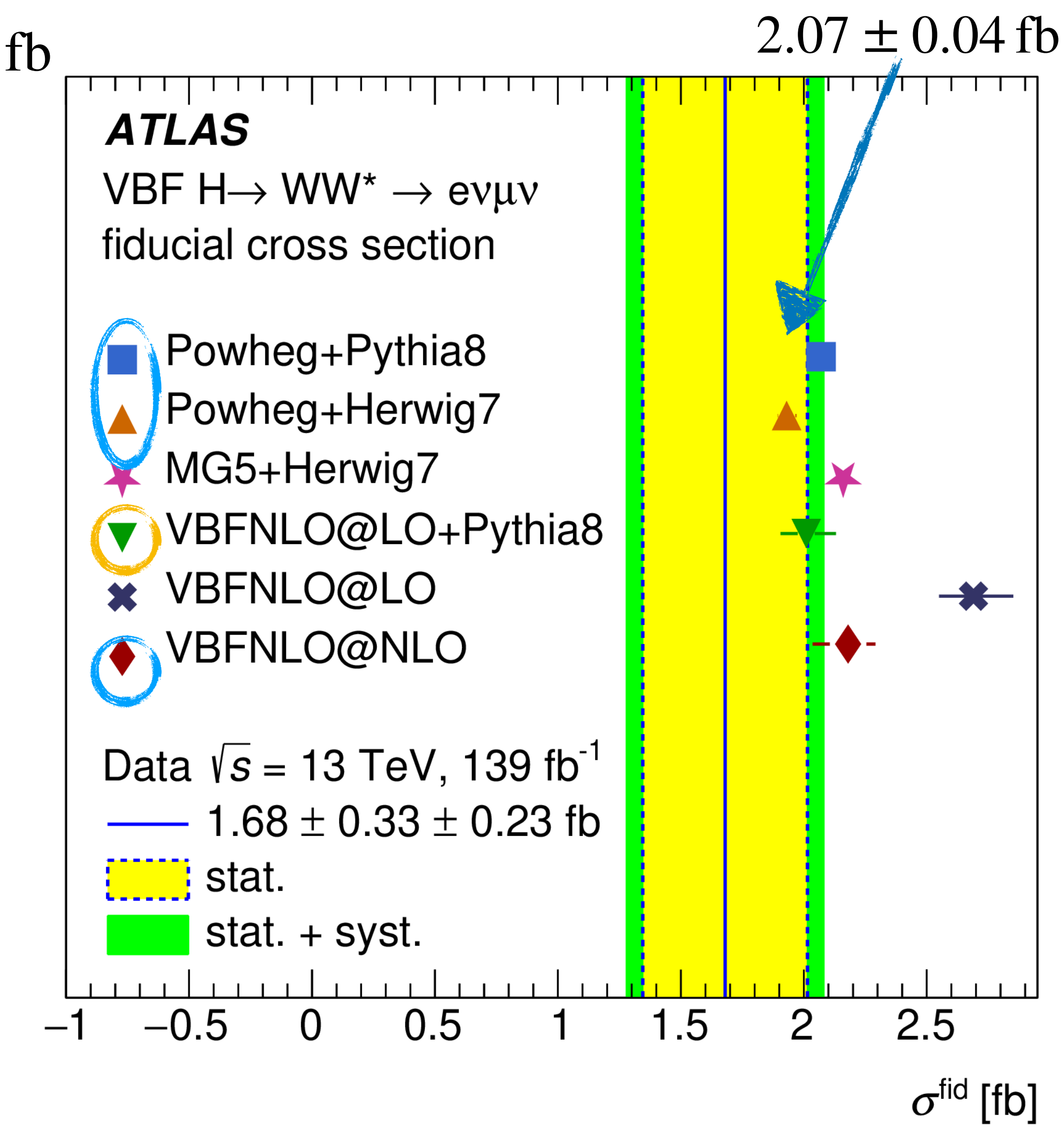

Consistent with SM predictions that include NLO QCD & EW corrections and with LO QCD calculation + PS

x-sections in VBF $H \to WW^* \to e\nu\mu\nu$

PRD 108, 072003

- Differential x-section measurements performed in **VBF-enriched region** ($N_{\rm jet} \geq 2$)
- Signal extracted from a simultaneous likelihood **fit of BDT discriminants** to data in several kinematic regions
- **13 observables** sensitive to the Higgs production and decay
  - $p_{\rm T}^{H}, p_{T}^{\ell\ell}, p_{T}^{\ell_1}, p_{T}^{\ell_2}, m_{\ell\ell}, |\Delta y_{\ell\ell}|, |\Delta\phi_{\ell\ell}|, \cos\theta_{\eta}^{*}, p_{T}^{j_1}, p_{T}^{j_2}, m_{jj}, |\Delta y_{jj}|, \Delta\phi_{jj}$
- Uncertainties driven by the data **statistical uncertainty**

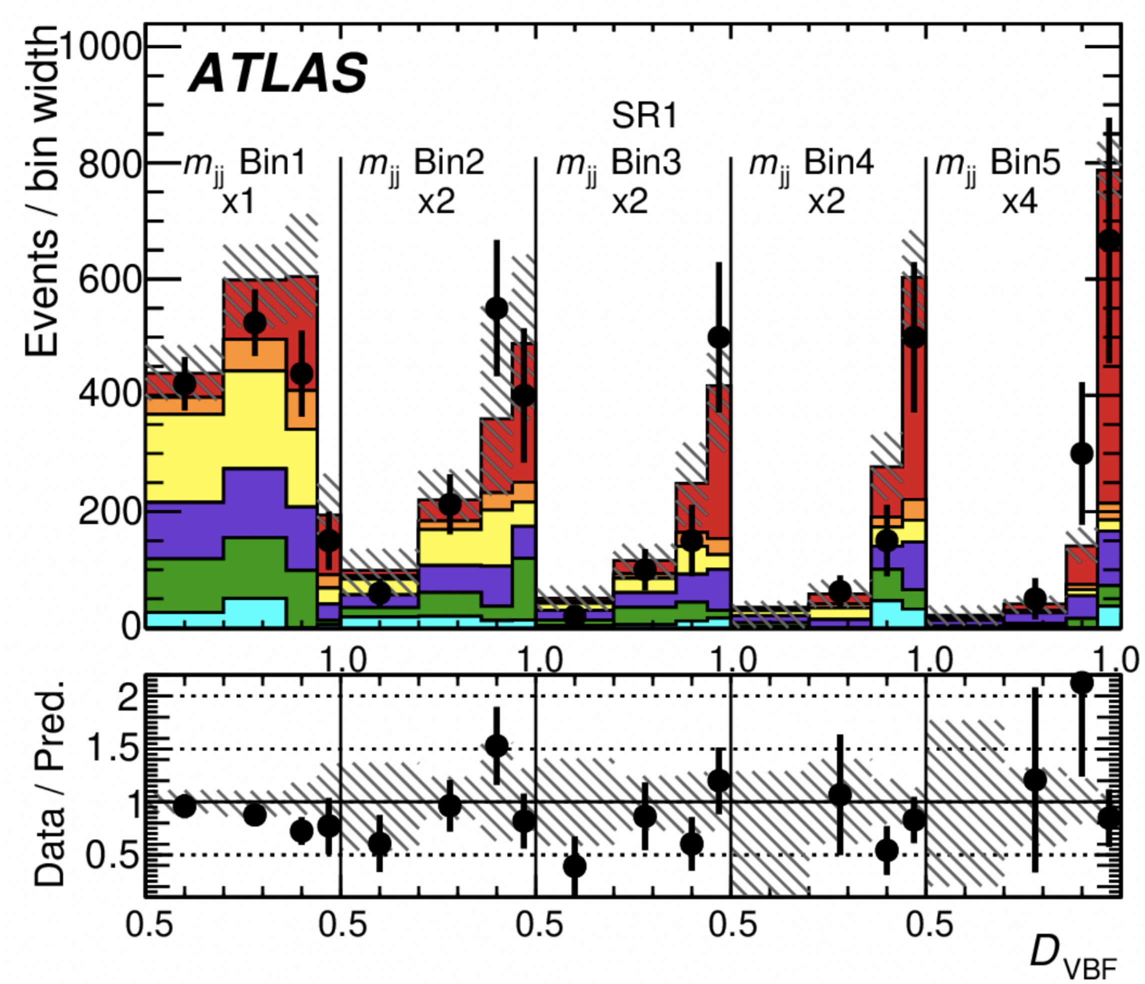

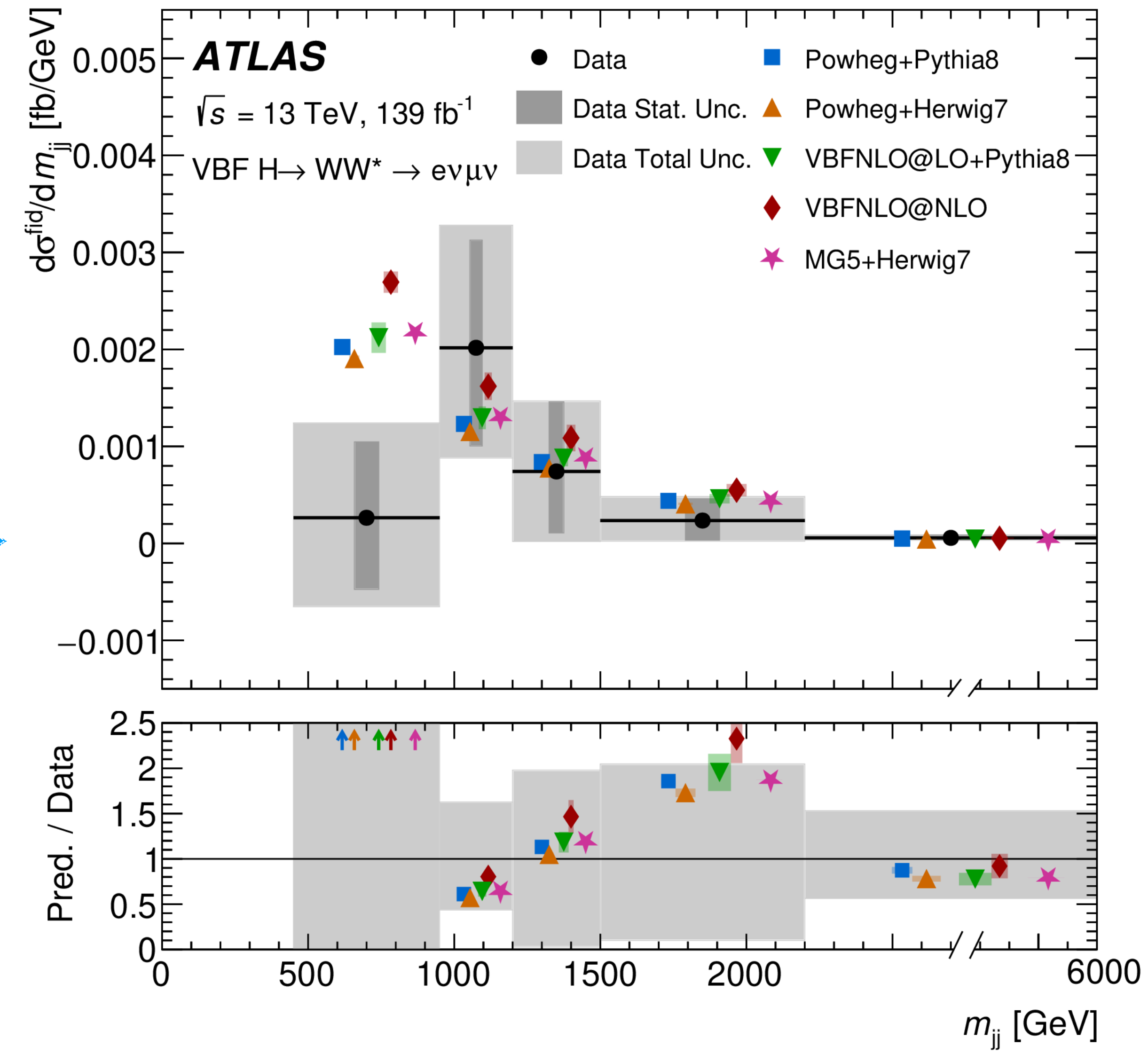

x-sections in VBF $H \to WW^* \to e\nu\mu\nu$ PRD 108, 072003

- Results also interpreted in **SMEFT framework**
- BSM interactions introduced via extra **higher-dimensional operators** $\mathcal{O}_i^{(d)}$ (only $d = 6$ considered)

$$\mathcal{L}_{\text{SMEFT}} = \mathcal{L}_{\text{SM}} + \sum_{i,d>4} \frac{C_i^{(d)}}{\Lambda^{d-4}} \mathcal{O}_i^{(d)}$$ where $C_i^{(d)}$ are Wilson coefficients and Λ represents new-physics scale

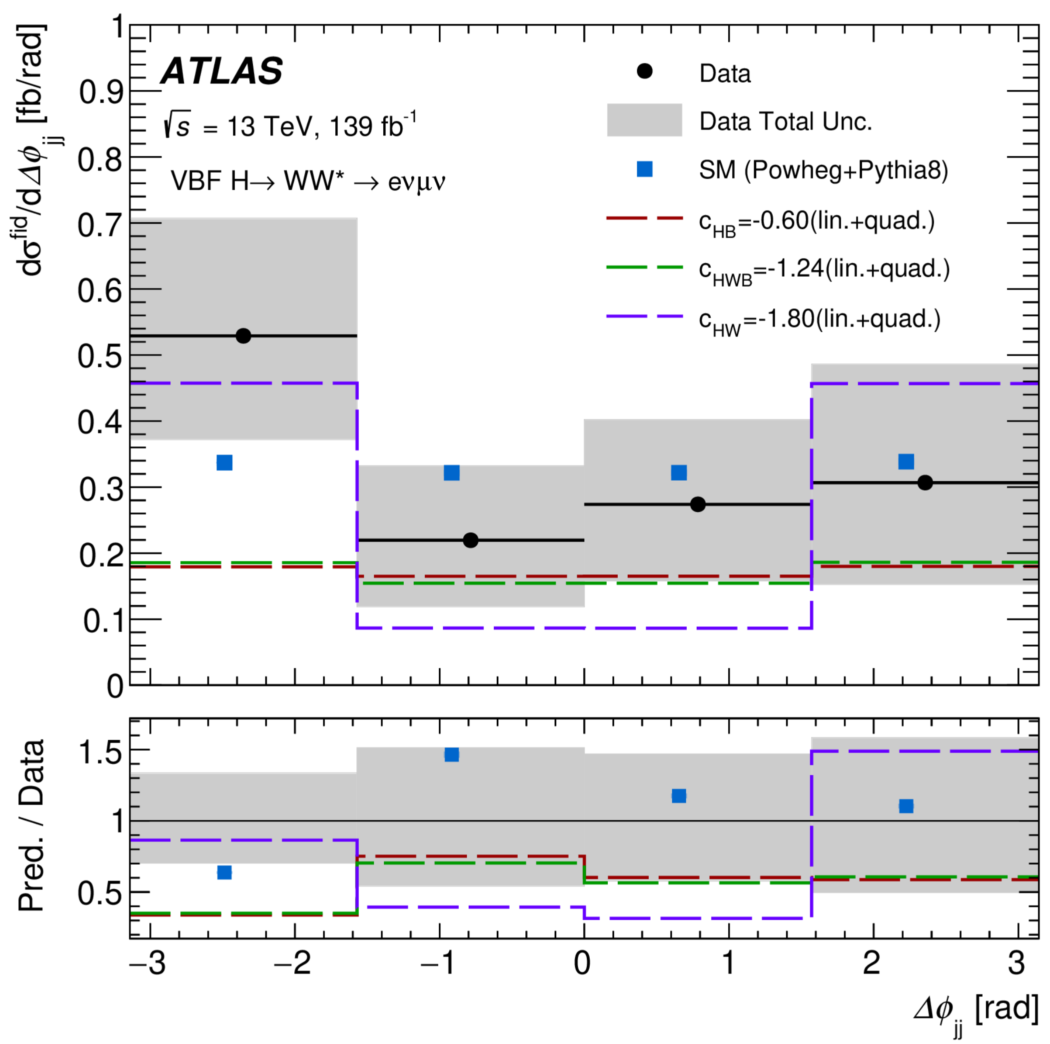

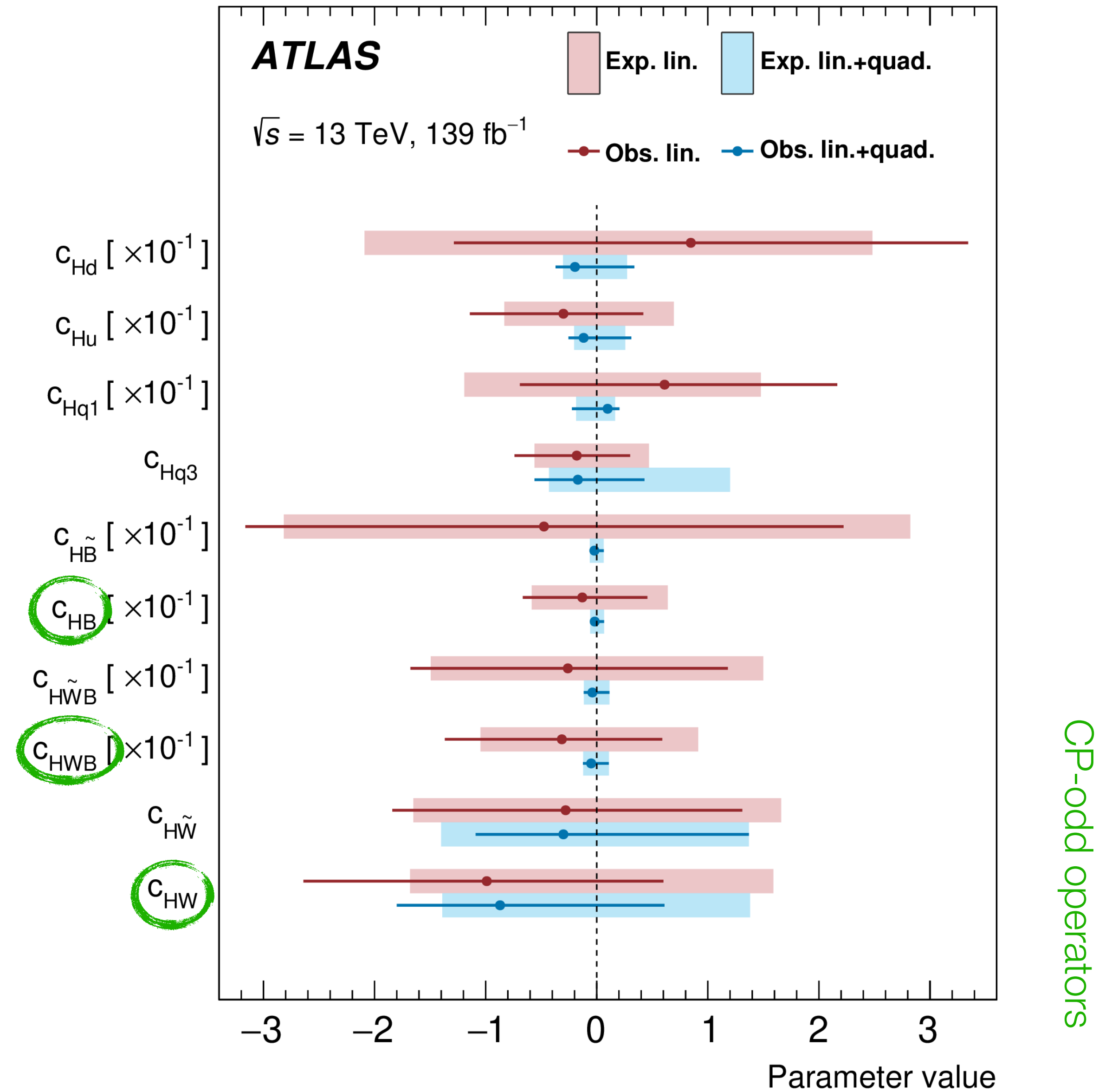

- Wilson coefficients constrained one at a time using the most sensitive differential distribution most sensitive

x-sections at 13.6 TeV

arXiv:2306.11379

- Inclusive production x-sections measured in two channels: $H \to ZZ^* \to 4\ell$ (29.0 ifb) and $H \to \gamma\gamma$ (31.4 ifb)
- Measured **fiducial x-sections** compatible with the SM predictions of 67.6 ± 3.7 fb ($\gamma\gamma$) and 3.67 ± 0.19 fb (4ℓ)
  - $\sigma^{\text{fid}}_{\gamma\gamma} = 76^{+14}_{-13}$ fb and $\sigma^{\text{fid}}_{4\ell} = 2.80 \pm 0.74$ fb
- **Extrapolated to the full phase space**, in agreement with the SM prediction of 59.9 ± 2.6 pb
  - $\sigma(pp \to H) = 58.2 \pm 7.5(\text{stat.}) \pm 4.5(\text{syst.})\text{ pb} = 58.2 \pm 8.7\text{ pb}$
- **Non-resonant backgrounds**
  - 4ℓ: constrained from dedicated data sidebands
  - $\gamma\gamma$: described by a function fitted to data
- Dominated by the **statistical uncertainty**
- Main **systematic uncertainties**: e and μ uncertainties (4ℓ), background modelling and photon efficiency ($\gamma\gamma$)

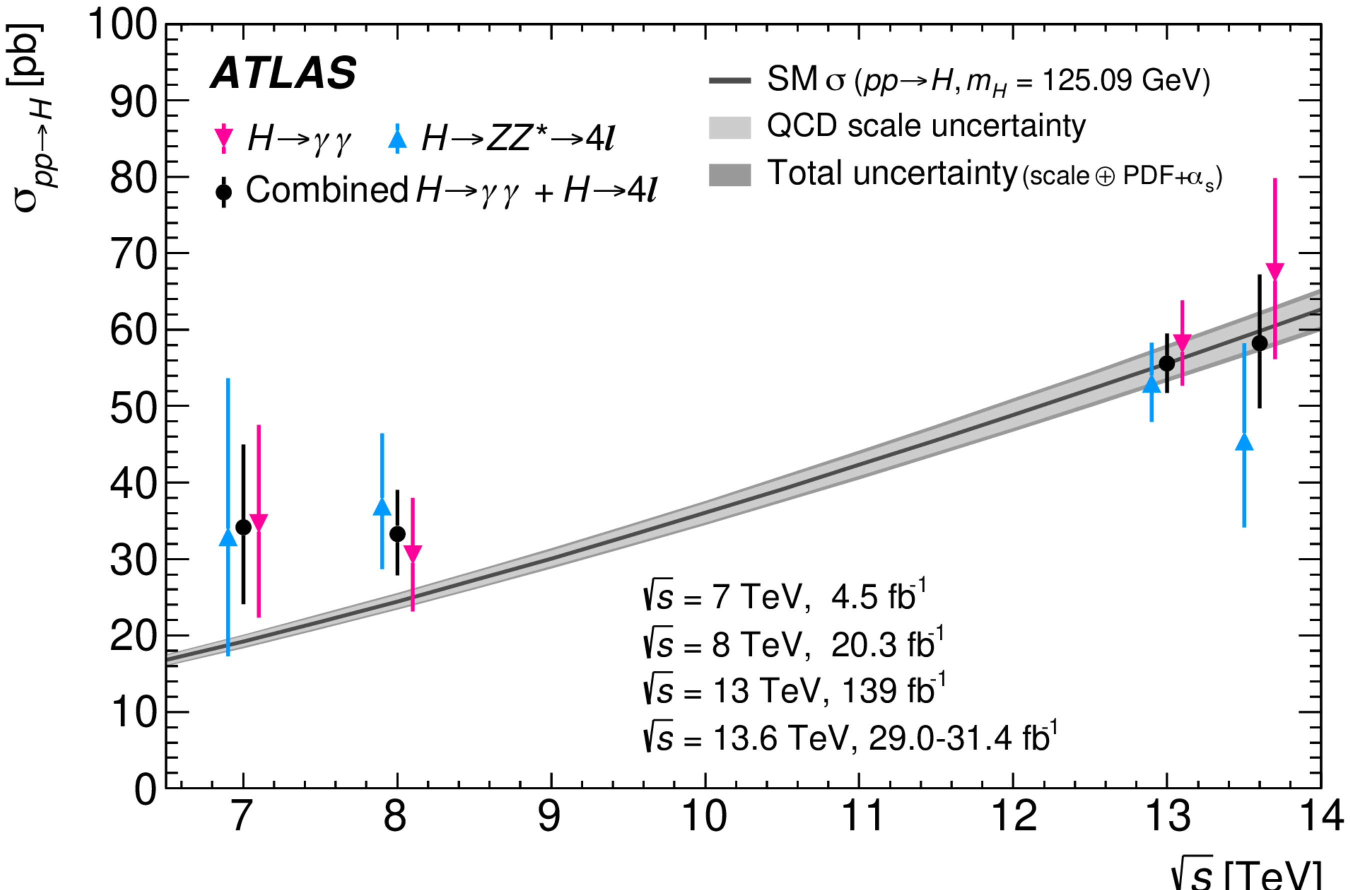

[1] Measurements restricted to a particle-level phase space closely matching detector-level kinematic selection, corrected for detector effects

Higgs boson mass

PLB 847 (2023) 138315

- m_H is a fundamental parameter in the SM, not predicted by the theory, crucial for determining other properties
- Measured in $H \to ZZ^* \to 4\ell$ and $H \to \gamma\gamma$ decay channels due to their excellent mass resolution (1-2%)
  - Fully reconstructable final states with a clean signature

- **Full Run 2 measurement in $H \to \gamma\gamma$ channel**
  - To increase the precision of the measurement, events are classified into 14 categories based on:
    - *Detector region*: central-barrel, outer-barrel and endcap
    - *Number of reconstructed converted photon candidates*: U-type (0) and C-type events (≥ 1)
    - $p_{Tt}^{\gamma\gamma}$: low, medium and high

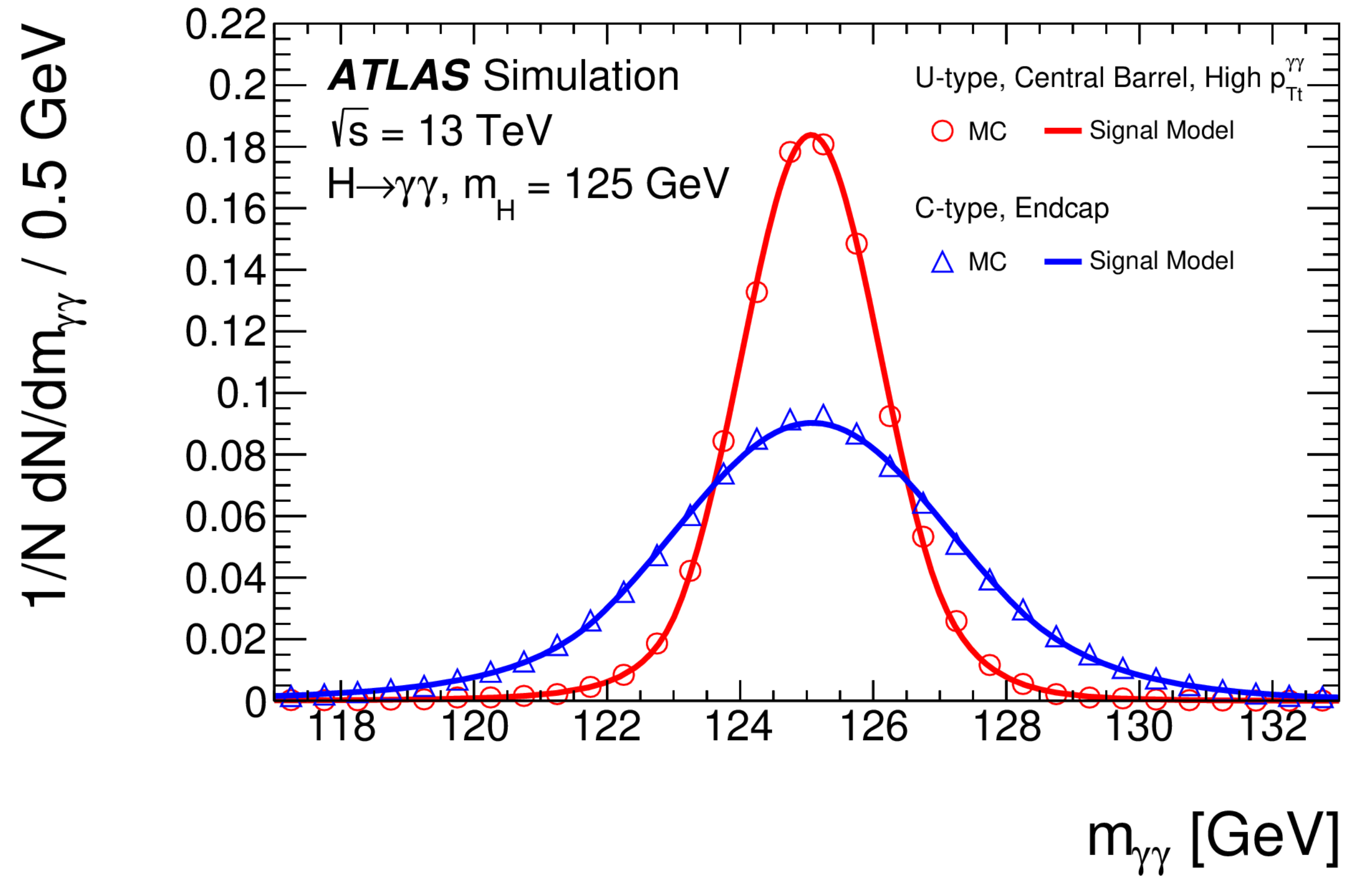

Higgs boson mass

PLB 847 (2023) 138315

- m_H is a fundamental parameter in the SM, not predicted by the theory, crucial for determining other properties
- Measured in $H \to ZZ^* \to 4\ell$ and $H \to \gamma\gamma$ decay channels due to their excellent mass resolution (1-2%)
  - Fully reconstructable final states with a clean signature

- **Full Run 2 measurement in $H \to \gamma\gamma$ channel**
  - Signal described by a *double-sided Crystal Ball* parametric in m_H
  - Background (non-resonant $\gamma\gamma$ production) represented by either an *exponential function*, a *power-law function* or an *exponentiated second-order polynomial* chosen by fitting $m_{\gamma\gamma}$
  - Systematic uncertainty reduced by a factor of 4 wrt the previous measurement based on partial Run 2 data

Improved photon energy scale calibration

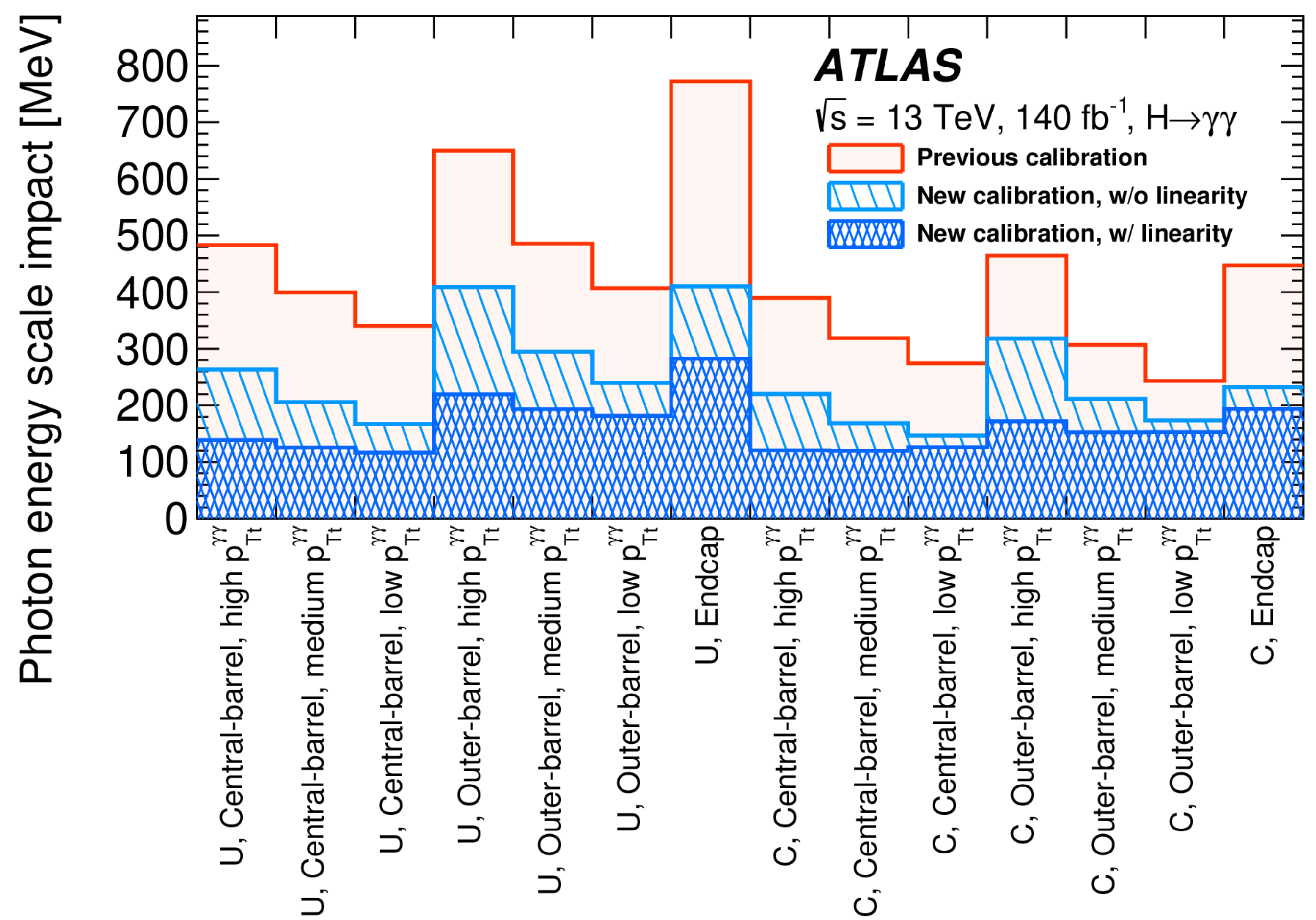

Higgs boson mass

PLB 847 (2023) 138315

- **Full Run 2 measurement in $H \to \gamma\gamma$ channel**
  - $0.1\,\%$ precision reached in a single channel

$$m_H = 125.17 \pm 0.11(\text{stat.}) \pm 0.09(\text{syst.})\,\text{GeV} = 125.17 \pm 0.14\,\text{GeV}$$

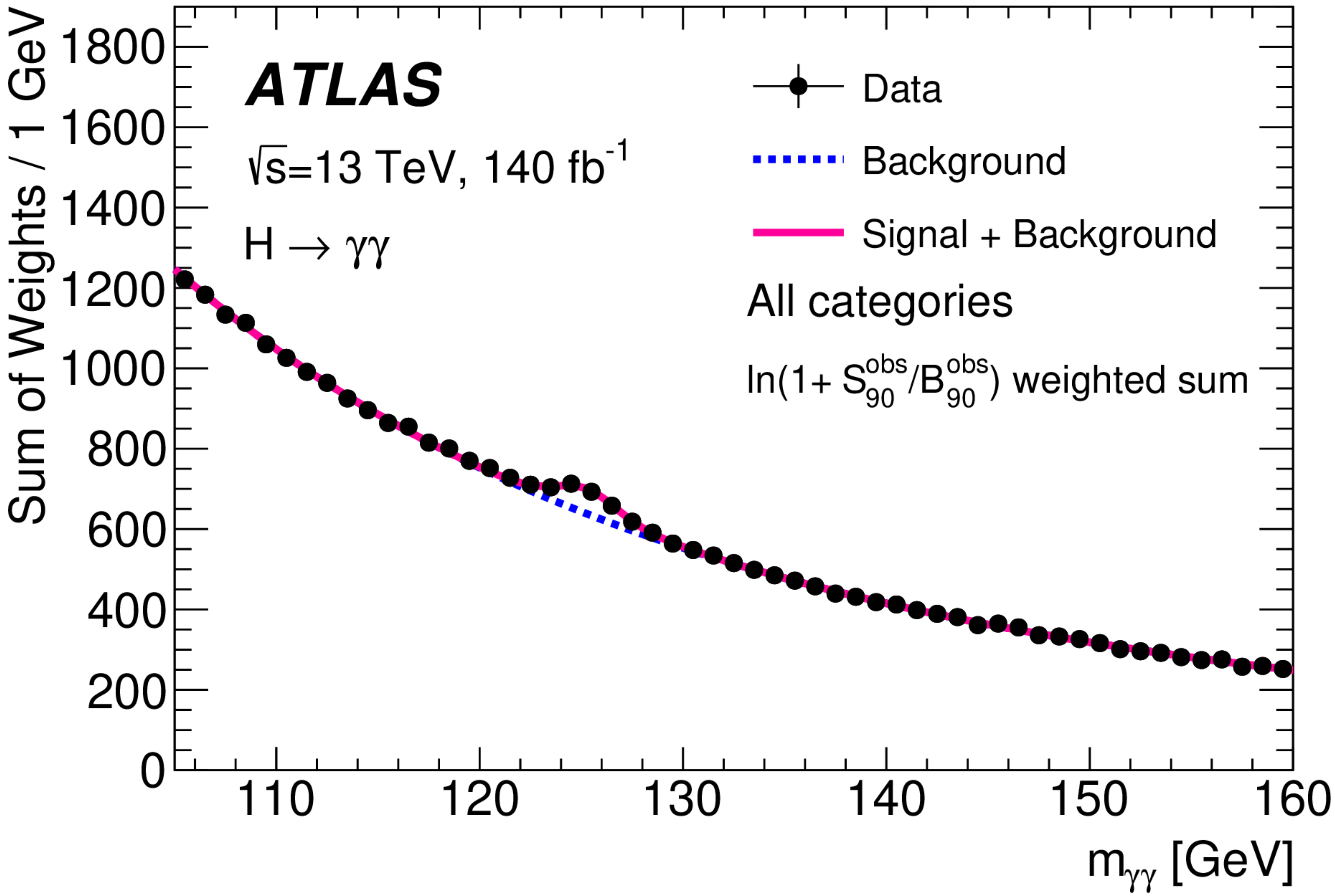

Higgs boson mass in $H \to \gamma\gamma$ and $H \to ZZ^* \to 4\ell$ arXiv:2308.04775

- Combination of Run 1 and Run 2 measurements in $H \to ZZ^* \to 4\ell$ and $H \to \gamma\gamma$ final states
- The most precise measurement of m_H up to date ($0.09\,\%$ precision):
  - $m_H = 125.10 \pm 0.09\,(\text{stat.}) \pm 0.06\,(\text{syst.})\,\text{GeV} = 125.11 \pm 0.11\,\text{GeV}$
- Dominant sources of systematic uncertainties associated to the electron and photon energy scales

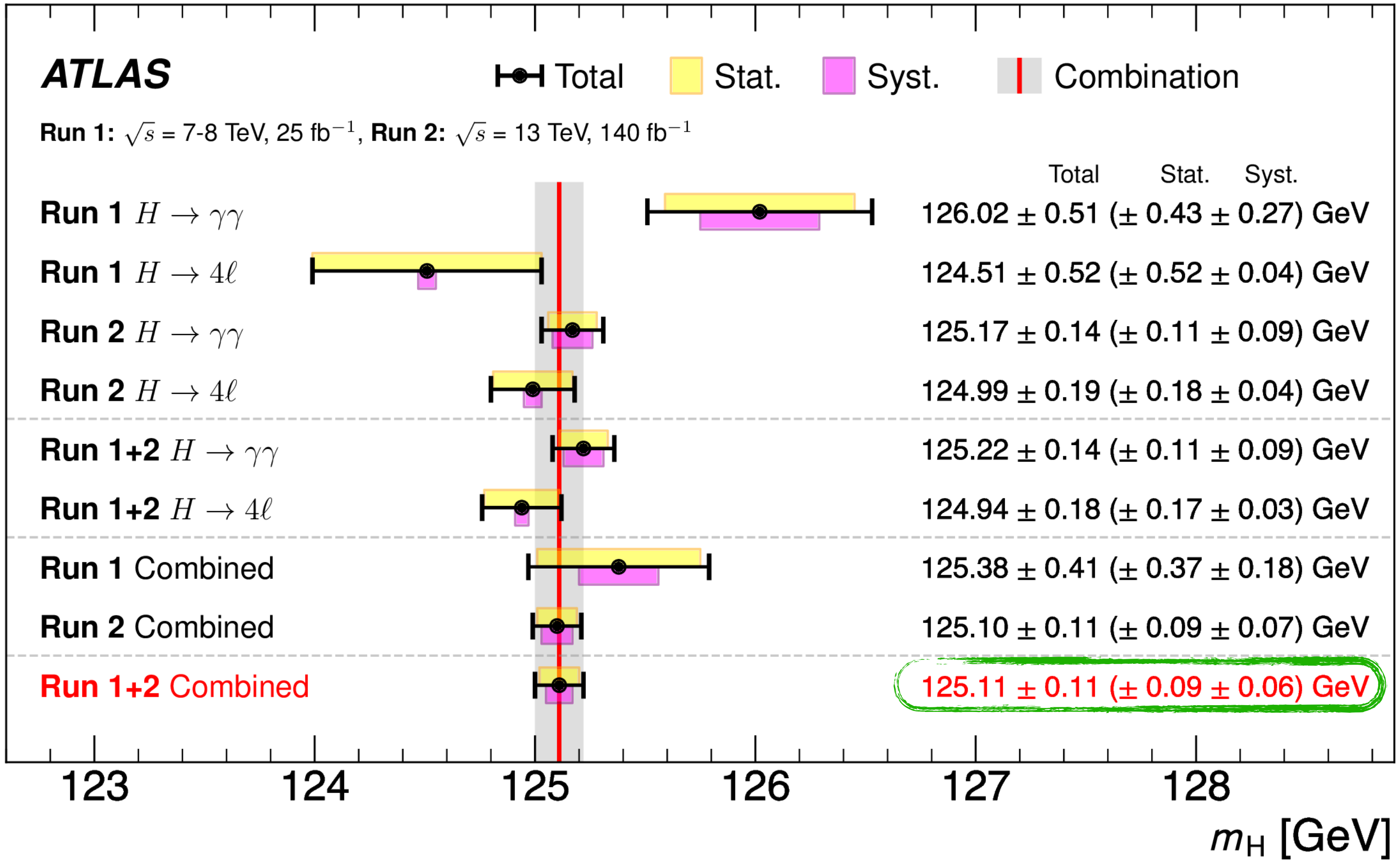

Higgs boson width

SM predicts the Higgs total width of 4.1 MeV

- Too *small for detector resolution*
- Can be obtained from the *ratio of on-shell and off-shell Higgs productions*

$$\sigma^{\text{on-shell}}_{gg\to H\to ZZ} \sim \frac{g^2_{ggH}g^2_{HZZ}}{m_H\Gamma_H}$$

$$\sigma^{\text{off-shell}}_{gg\to H\to ZZ} \sim \frac{g^2_{ggH}g^2_{HZZ}}{m^2_{ZZ}}$$

$$\Rightarrow\ \sigma^{\text{off-shell}}_{gg\to H\to ZZ}/\sigma^{\text{on-shell}}_{gg\to H\to ZZ} \sim \Gamma_H$$

- Assuming that the on-shell and off-shell couplir constants evolve like in SM
- The **interference** between the **signal** and **background** is large and destructive

Theoretical line-shape (narrow relativistic Breit-Wigner distribution)

convoluted with the detector response

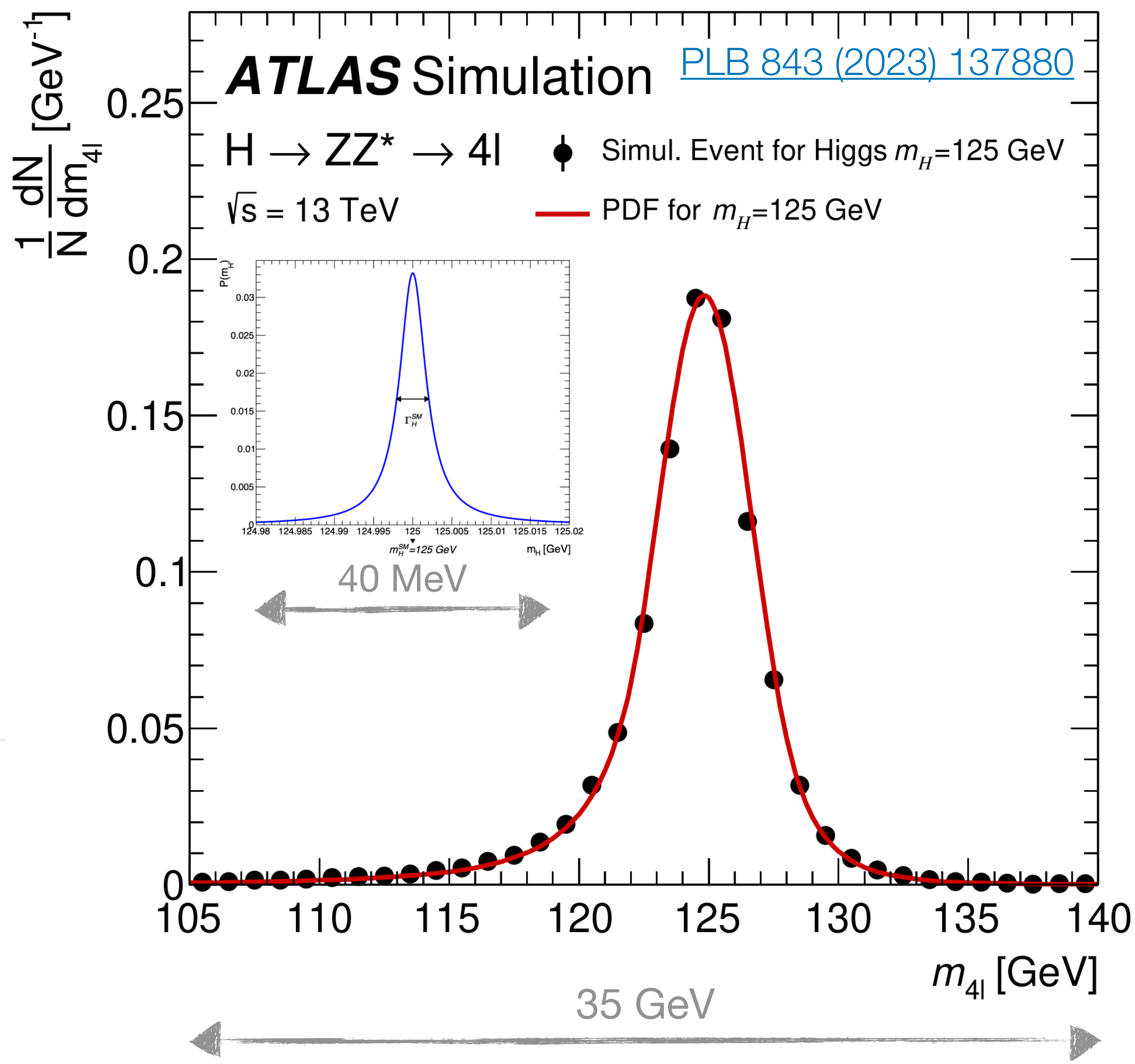

Higgs boson width

SM predicts the **Higgs total width of 4.1 MeV**

- *Too small for detector resolution*
- Can be obtained from the *ratio of on-shell and off-shell Higgs productions*

$$\sigma^{\text{on-shell}}_{gg\to H\to ZZ} \sim \frac{g^2_{ggH} g^2_{HZZ}}{m_H \Gamma_H}$$

$$\sigma^{\text{off-shell}}_{gg\to H\to ZZ} \sim \frac{g^2_{ggH} g^2_{HZZ}}{m^2_{ZZ}}$$

$$\Rightarrow \sigma^{\text{off-shell}}_{gg\to H\to ZZ} / \sigma^{\text{on-shell}}_{gg\to H\to ZZ} \sim \Gamma_H$$

- Assuming that the on-shell and off-shell coupling constants evolve like in SM
- The **interference** between the **signal** and **background** is large and destructive

Krauer and Passarino

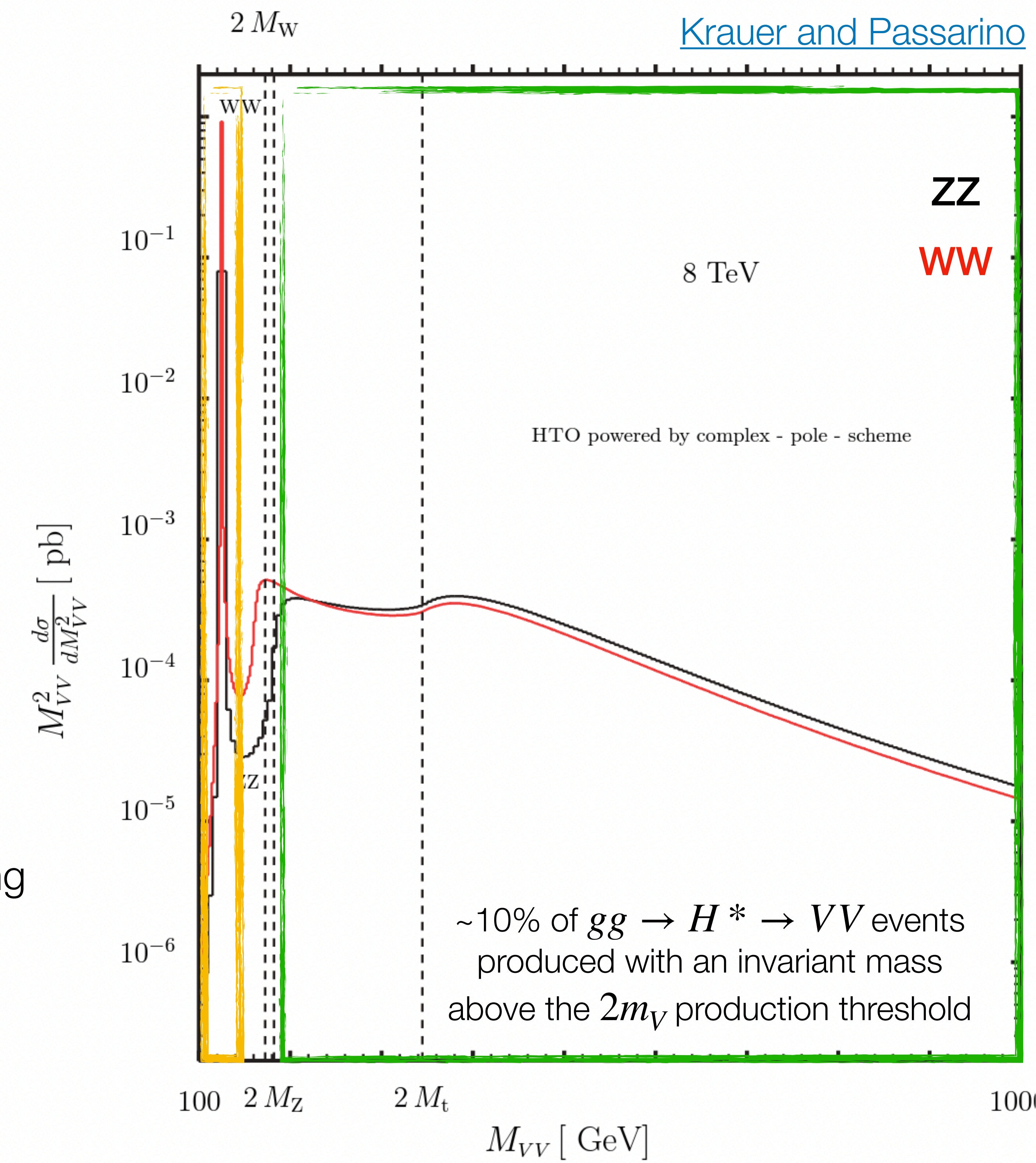

~10% of $gg \to H^* \to VV$ events produced with an invariant mass above the $2m_V$ production threshold

Higgs boson width

SM predicts the **Higgs total width of 4.1 MeV**

- Too *small for detector resolution*
- Can be obtained from the *ratio of on-shell and off-shell Higgs productions*

$$\sigma^{\text{on-shell}}_{gg\to H\to ZZ} \sim \frac{g^2_{ggH} g^2_{HZZ}}{m_H \Gamma_H}$$

$$\sigma^{\text{off-shell}}_{gg\to H\to ZZ} \sim \frac{g^2_{ggH} g^2_{HZZ}}{m^2_{ZZ}}$$

$$\Rightarrow \ \sigma^{\text{off-shell}}_{gg\to H\to ZZ} / \sigma^{\text{on-shell}}_{gg\to H\to ZZ} \sim \Gamma_H$$

- Assuming that the on-shell and off-shell coupling constants evolve like in SM
- The **interference** between the **signal** and **background** is large and destructive

EPJC (2015) 71:335

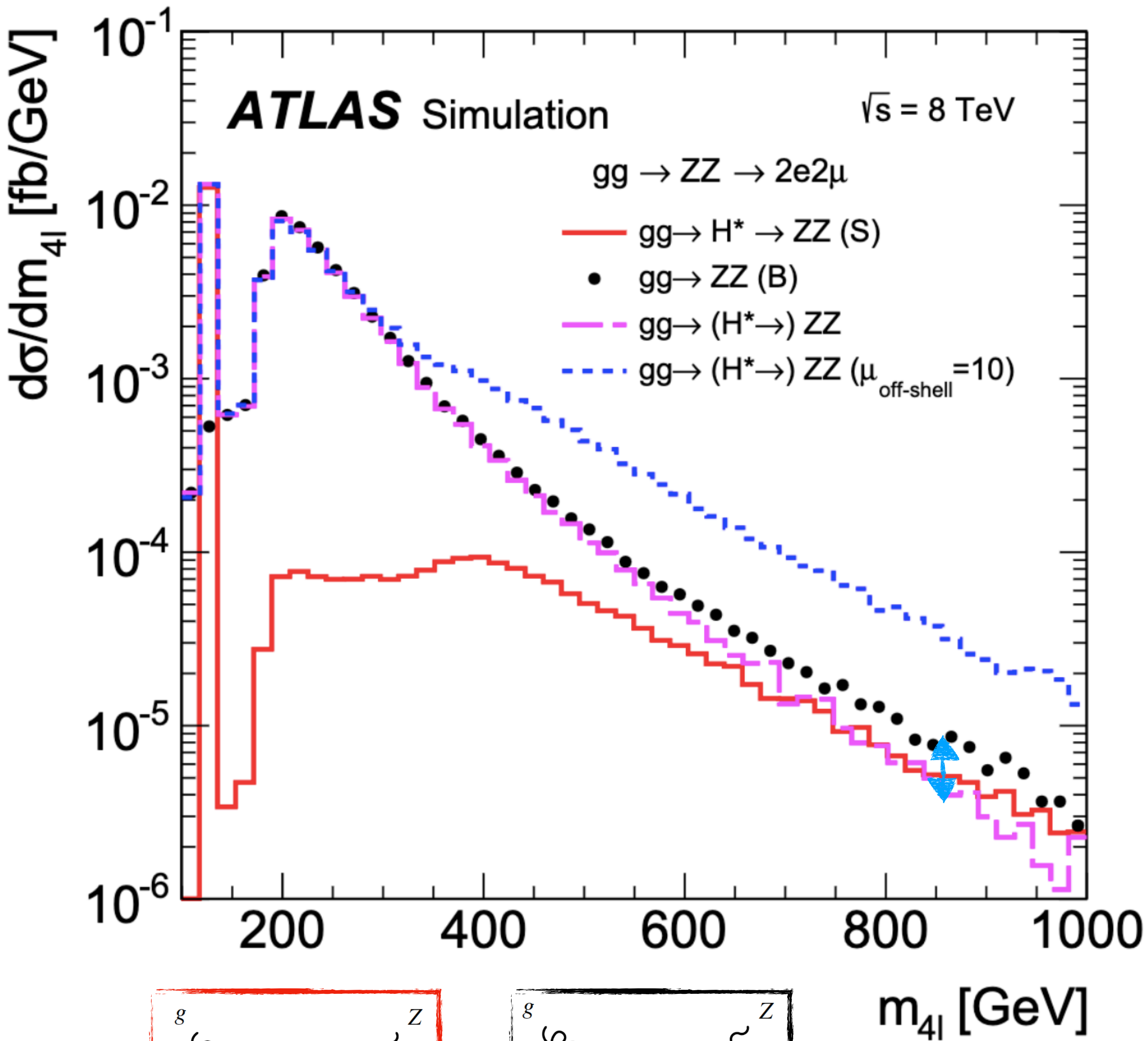

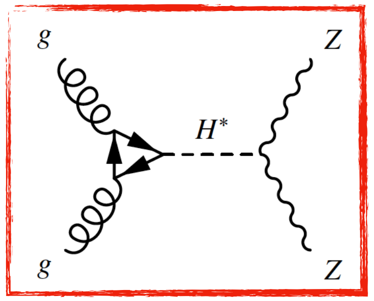

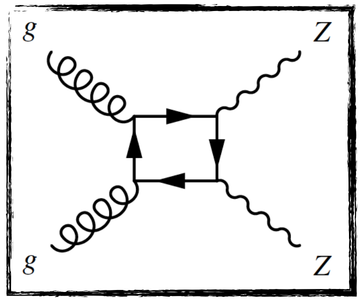

$$N = \mu S + \sqrt{\mu} I + \mathbf{B}$$

Higgs boson width in $H^* \to ZZ \to 4\ell/2\ell 2\nu$ PLB 846 (2023) 138223

- **Full Run 2 measurement**
  - Observables
    - 4ℓ: built from NN outputs trained with kinematic information of the four lepton from MC simulation and also the square of the modulus of the values of the LO ME
    - $2\ell 2\nu$: transverse mass of the ZZ system
  - Signal regions: defined as $m_{4\ell} > 220$ GeV
    - **EW SR**: $n_{\text{jets}} \geq 2$ and $|\Delta\eta_{jj}| > 4.0$
    - **Mixed SR**: $n_{\text{jets}} = 1$ and $\eta_j > 2.2$
    - **ggF SR**: remaining events

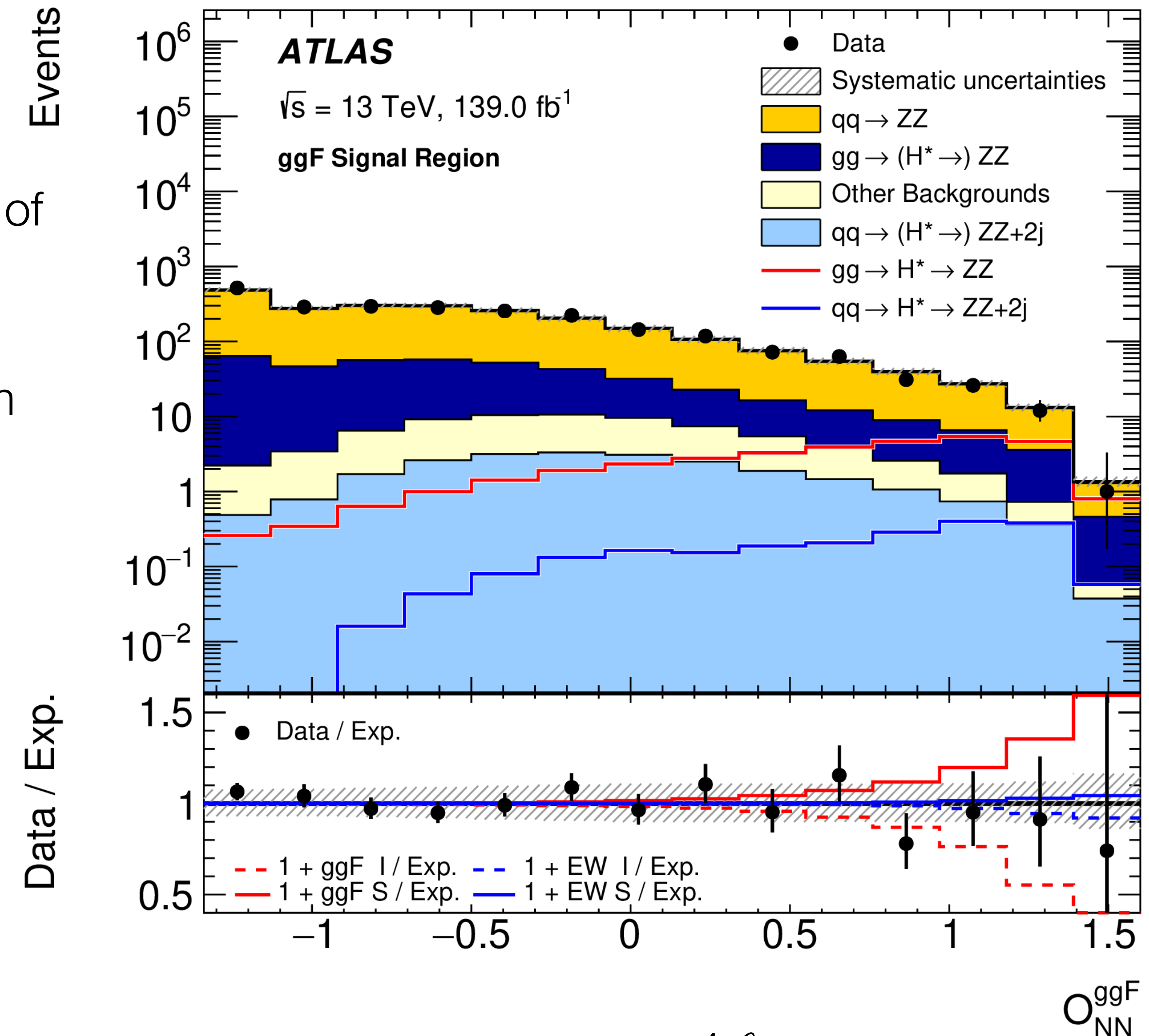

ggF SR in the 4ℓ channel

Higgs boson width in $H^* \rightarrow ZZ \rightarrow 4\ell/2\ell 2\nu$

PLB 846 (2023) 138223

ATL-PHYS-PUB-2023-012

- **Full Run 2 measurement**
  - Each background has a dedicated control region and a floating normalisation in the fit
  - Main systematic uncertainties:
    - Exp: parton shower (QSF, CKKW), jet-related uncertainties
    - Theory: high-order corrections
  - Statistically limited measurement: $\Gamma_H = 4.5^{+3.3}_{-2.5}\,\mathrm{MeV}$
  - Background-only hypothesis rejected with $3.3\,\sigma$ significance $\Rightarrow$ evidence for the off-shell Higgs production
  - Results also interpreted in **SMEFT framework**

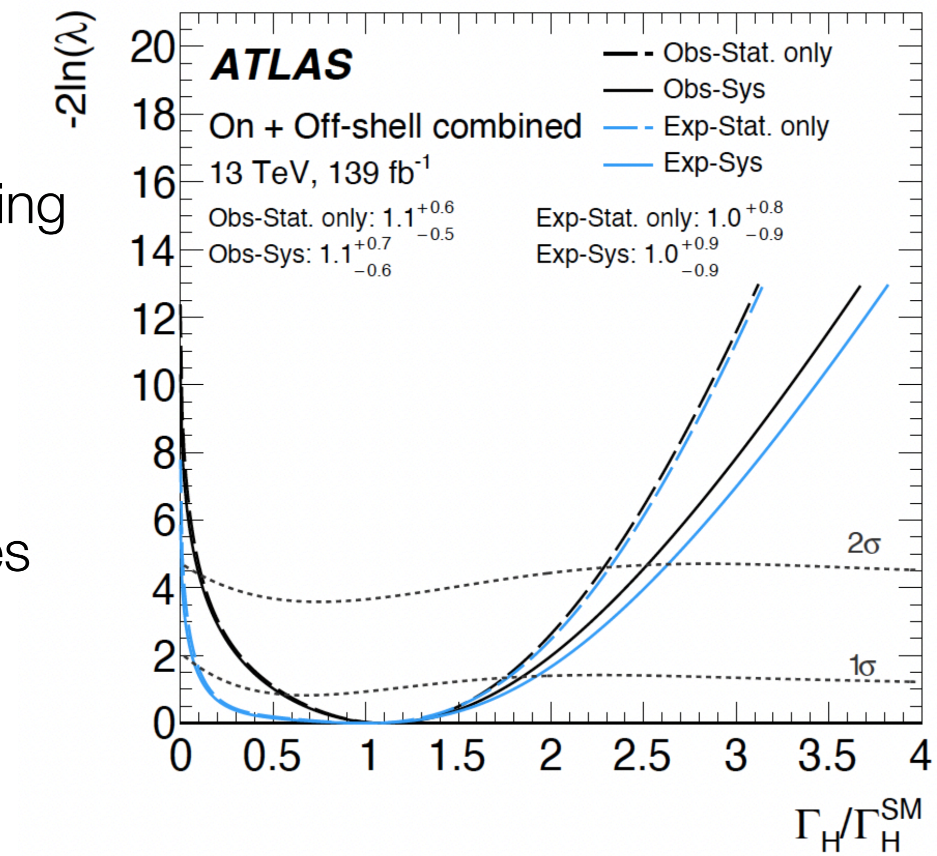

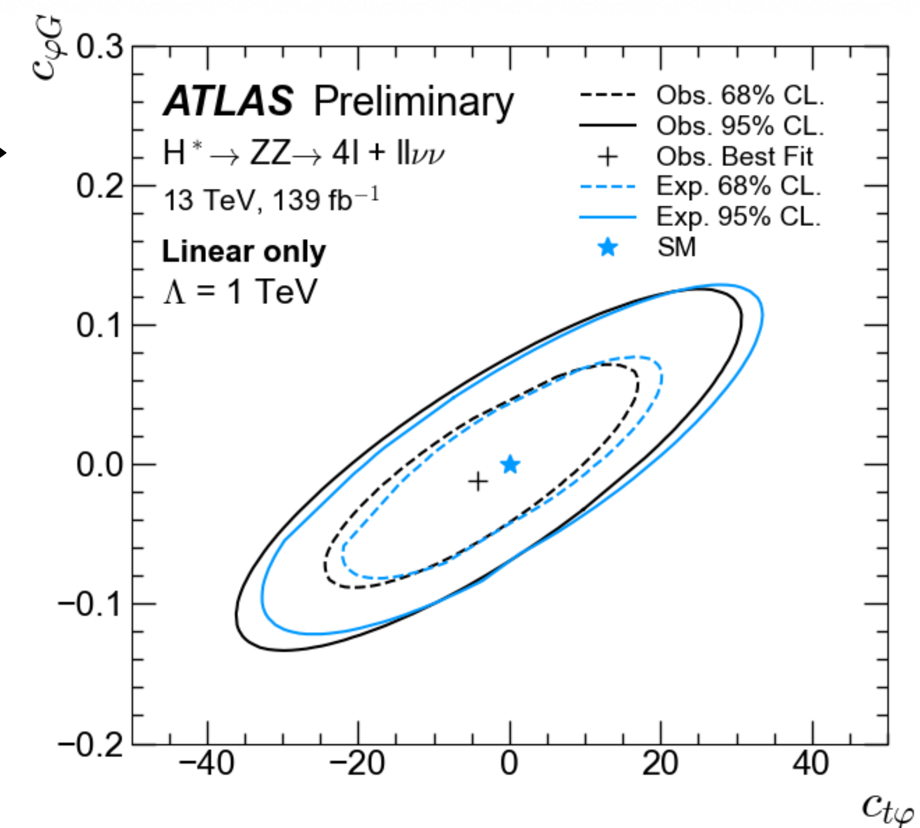

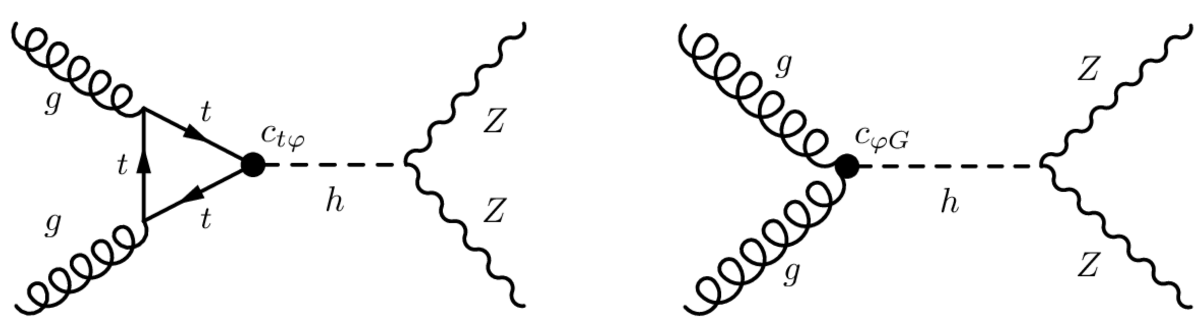

Conclusion

- With Run 1 and Run 2 data, we are entering the **era of precision measurements** of the Higgs properties
  - ~6% precision on the **inclusive Higgs boson production cross-section** [Nature 607, 52 (2022)]
  - 7-12% precision on the **Higgs boson couplings** to the three heaviest fermions (t, b, τ) [Nature 607, 52 (2022)]
  - ~5% precision on the Higgs boson couplings to the weak bosons (W, Z) [Nature 607, 52 (2022)]
  - 0.09% precision on the **Higgs boson mass** [PLB 847 (2023) 138315], [arXiv:2308.04775]
  - ~60% precision on the **Higgs boson total width** [PLB 846 (2023) 138223]
- **Differential cross-sections** measured in several channels and sensitive variables [EPJC 83 (2023) 774], [PRD 108, 072003]
  - Results in a **good agreement with the SM** predictions
  - Generally dominated by **statistical uncertainties**
- **First Run 3 measurements** of the fiducial and total production cross-sections with 2022 data [arXiv:2306.11379]
  - Potential to significantly **improve accuracy and achieve sensitivity** to rare processes
  - See talk Prospects for single- and di-Higgs measurements at the HL-LHC (ATLAS and CMS) by Lei Zhang later today

Conclusion

- With Run 1 and Run 2 data, we are entering the **era of precision measurements** of the Higgs properties
  - ~6% precision on the **inclusive Higgs boson production cross-section** [Nature 607, 52 (2022)]
  - 7-12% precision on the **Higgs boson couplings** to the three heaviest fermions (t, b, τ) [Nature 607, 52 (2022)]
  - ~5% precision on the Higgs boson couplings to the weak bosons (W, Z) [Nature 607, 52 (2022)]
  - 0.09
  - ~60
- **Differential cross-sections** measured in several channels and sensitive variables [EPJC 83 (2023) 774], [PRD 108, 072003]
  - Results in a **good agreement with the SM** predictions
  - Generally dominated by **statistical uncertainties**
- **First Run 3 measurements** of the fiducial and total production cross-sections with 2022 data [arXiv:2306.11379]
  - Potential to significantly **improve accuracy and achieve sensitivity** to rare processes
  - See talk Prospects for single- and di-Higgs measurements at the HL-LHC (ATLAS and CMS) by Lei Zhang later today

Thank you for your attention and stay tuned for new results!

BACKUP

Higgs boson

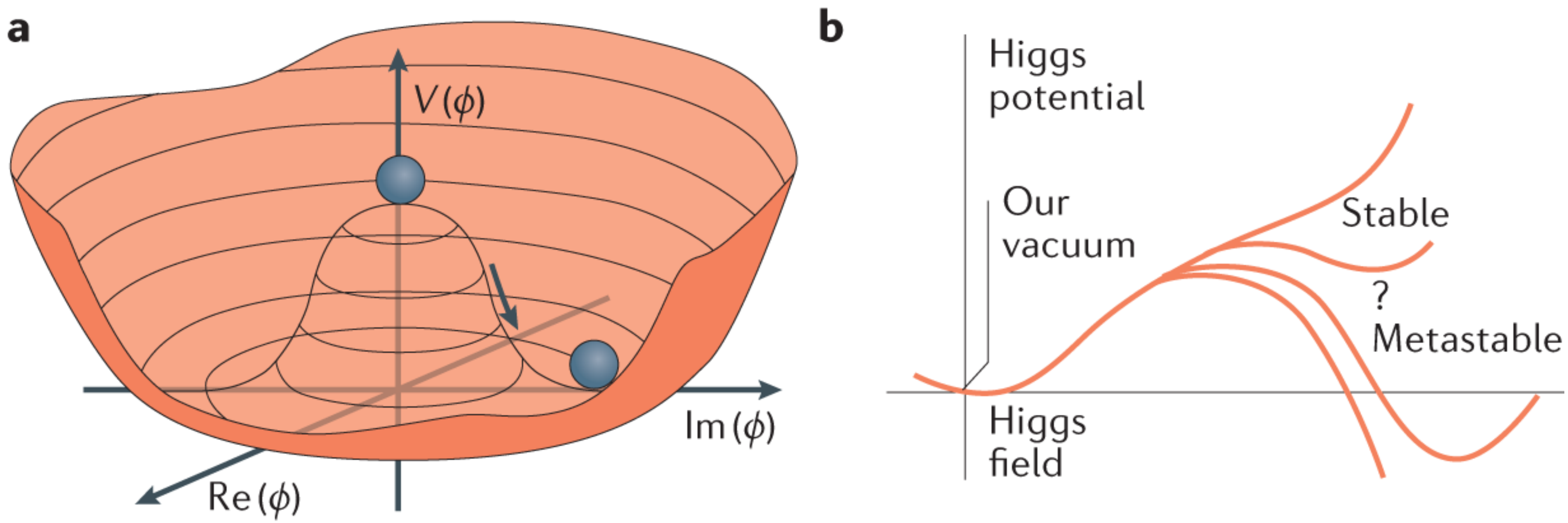

[Nature Reviews Physics volume 3, pages 608–624 (2021)]

LHC: interactions per crossing

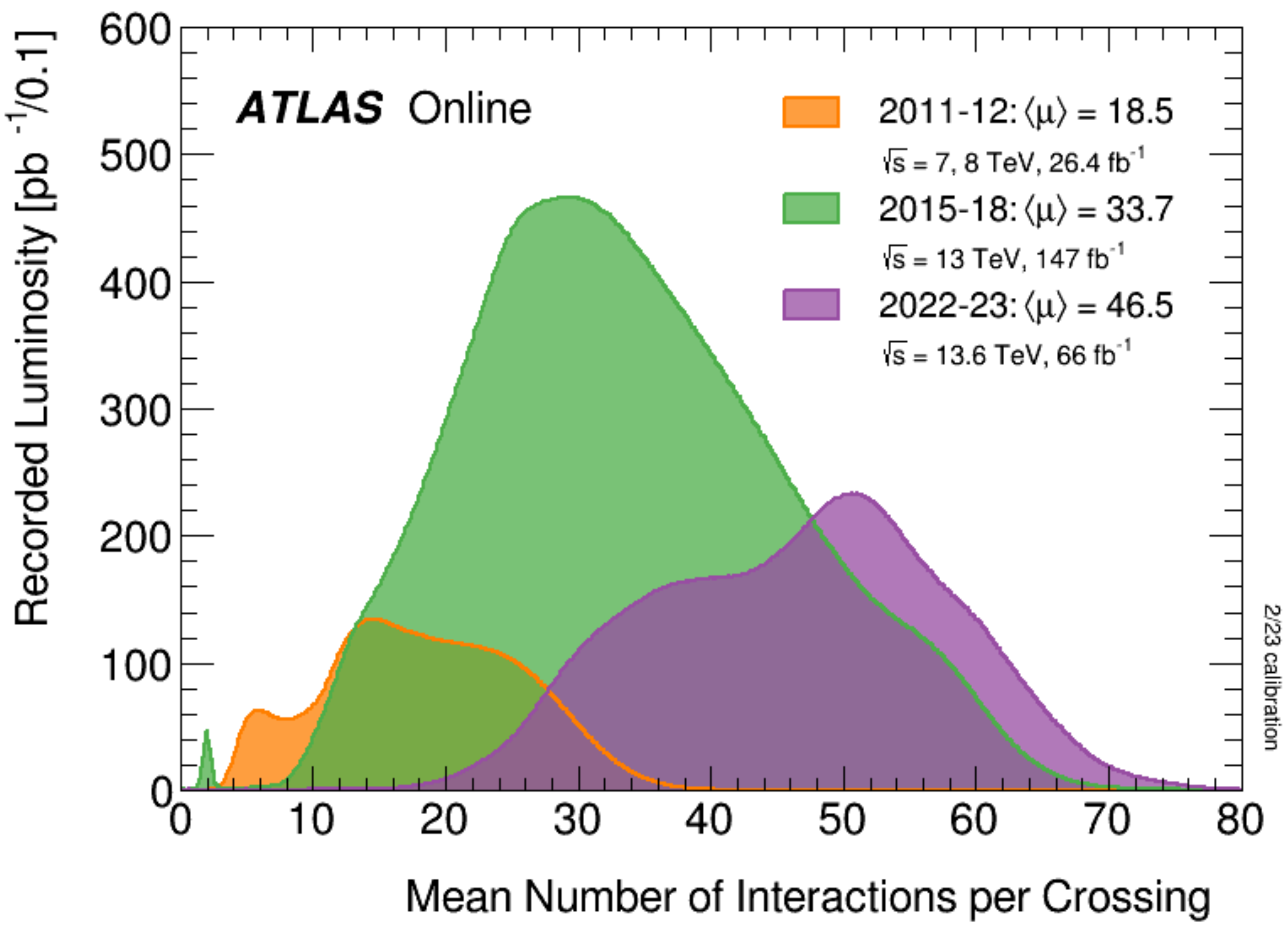

[Public ATLAS Luminosity Results]

Higgs boson production and decay

Nature 607, 52 (2022)

	(a) $B_{inv.} = B_{u.} = 0$	(b) $B_{inv.}$ free, $B_{u.} \geq 0$, $\kappa_{W,Z} \leq 1$
κ_Z	$0.99^{+0.06}_{-0.06}$	$0.98^{+0.02}_{-0.05}$
κ_W	$1.05^{+0.06}_{-0.06}$	$1.00_{-0.02}$
κ_t	$0.94^{+0.11}_{-0.11}$	$0.94^{+0.11}_{-0.11}$
κ_b	$0.89^{+0.11}_{-0.11}$	$0.82^{+0.09}_{-0.08}$
κ_τ	$0.93^{+0.07}_{-0.07}$	$0.91^{+0.07}_{-0.06}$
κ_μ	$1.06^{+0.25}_{-0.30}$	$1.04^{+0.23}_{-0.30}$
κ_g	$0.95^{+0.07}_{-0.07}$	$0.94^{+0.07}_{-0.06}$
κ_γ	$1.01^{+0.06}_{-0.06}$	$0.98^{+0.05}_{-0.05}$
$\kappa_{Z\gamma}$	$1.38^{+0.31}_{-0.37}$	$1.35^{+0.29}_{-0.36}$
$B_{inv.}$	-	< 0.13
$B_{u.}$	-	< 0.12

Measured Higgs boson coupling modifiers per particle type

Higgs boson production and decay **Nature 607, 52 (2022)**

Production cross section	Effective coupling	Parametrization in terms of coupling strength modifiers
$\sigma(\text{ggF})$	κ_g^2	$1.040\,\kappa_t^2 + 0.002\,\kappa_b^2 - 0.038\,\kappa_t\kappa_b - 0.005\,\kappa_t\kappa_c$
$\sigma(\text{VBF})$	-	$0.733\,\kappa_W^2 + 0.267\,\kappa_Z^2$
$\sigma(qq/qg \to ZH)$	-	κ_Z^2
$\sigma(gg \to ZH)$	-	$2.456\,\kappa_Z^2 + 0.456\,\kappa_t^2 - 1.903\,\kappa_Z\kappa_t - 0.011\,\kappa_Z\kappa_b + 0.003\,\kappa_t\kappa_b$
$\sigma(WH)$	-	κ_W^2
$\sigma(t\bar{t}H)$	-	κ_t^2
$\sigma(tHW)$	-	$2.909\,\kappa_t^2 + 2.310\,\kappa_W^2 - 4.220\,\kappa_t\kappa_W$
$\sigma(tHq)$	-	$2.633\,\kappa_t^2 + 3.578\,\kappa_W^2 - 5.211\,\kappa_t\kappa_W$
$\sigma(b\bar{b}H)$	-	κ_b^2
Partial decay width		
Γ^{bb}	-	κ_b^2
Γ^{WW}	-	κ_W^2
Γ^{gg}	κ_g^2	$1.111\,\kappa_t^2 + 0.012\,\kappa_b^2 - 0.123\,\kappa_t\kappa_b$
$\Gamma^{\tau\tau}$	-	κ_τ^2
Γ^{ZZ}	-	κ_Z^2
Γ^{cc}	-	$\kappa_c^2\ (= \kappa_t^2)$
$\Gamma^{\gamma\gamma}$	κ_γ^2	$1.589\,\kappa_W^2 + 0.072\,\kappa_t^2 - 0.674\,\kappa_W\kappa_t$ $+0.009\,\kappa_W\kappa_\tau + 0.008\,\kappa_W\kappa_b - 0.002\,\kappa_t\kappa_b - 0.002\,\kappa_t\kappa_\tau$
$\Gamma^{Z\gamma}$	$\kappa_{Z\gamma}^2$	$1.118\,\kappa_W^2 - 0.125\,\kappa_W\kappa_t + 0.004\,\kappa_t^2 + 0.003\,\kappa_W\kappa_b$
Γ^{ss}	-	$\kappa_s^2\ (= \kappa_b^2)$
$\Gamma^{\mu\mu}$	-	κ_μ^2
Total width ($B_{\text{inv.}} = B_{\text{u.}} = 0$)		
Γ_H	κ_H^2	$0.581\,\kappa_b^2 + 0.215\,\kappa_W^2 + 0.082\,\kappa_g^2 + 0.063\,\kappa_\tau^2 + 0.026\,\kappa_Z^2 + 0.029\,\kappa_c^2$ $+0.0023\,\kappa_\gamma^2 + 0.0015\,\kappa_{Z\gamma}^2 + 0.0004\,\kappa_s^2 + 0.00022\,\kappa_\mu^2$

Parametrisations of Higgs boson production cross sections, partial decay widths, and the total width, normalised to their SM values, as functions of the coupling strength modifiers κ

Higgs boson production and decay

Nature 607, 52 (2022)

STXS	Cross section [pb]	SM prediction [pb]
$gg \to H$, 0-jet, $p_T^H < 10$ GeV	$5.8 \pm 1.3(^{+1.2}_{-1.1}(stat.)^{+0.7}_{-0.6}(syst.))$	6.6 ± 0.9
$gg \to H$, 0-jet, $10 \le p_T^H < 200$ GeV	$25.4^{+2.7}_{-2.6}(\pm 1.8(stat.)^{+2.0}_{-1.8}(syst.))$	20.6 ± 1.5
$gg \to H$, 1-jet, $p_T^H < 60$ GeV	$5.2 \pm 1.7(\pm 1.3(stat.) \pm 1.1(syst.))$	6.5 ± 0.9
$gg \to H$, 1-jet, $60 \le p_T^H < 120$ GeV	$5.5^{+1.2}_{-1.1}(\pm 1.0(stat.)^{+0.7}_{-0.6}(syst.))$	4.5 ± 0.6
$gg \to H$, 1-jet, $120 \le p_T^H < 200$ GeV	$0.73^{+0.30}_{-0.29}(\pm 0.25(stat.)^{+0.16}_{-0.14}(syst.))$	0.75 ± 0.13
$gg \to H$, $\ge$ 2-jet, $m_{jj} < 350$ GeV, $p_T^H < 120$ GeV	$1.2 \pm 1.4(\pm 1.2(stat.) \pm 0.7(syst.))$	3.0 ± 0.6
$gg \to H$, $\ge$ 2-jet, $m_{jj} < 350$ GeV, $120 \le p_T^H < 200$ GeV	$0.9 \pm 0.4(\pm 0.4(stat.) \pm 0.2(syst.))$	0.94 ± 0.22
$gg \to H$, $\ge$ 2-jet, $m_{jj} \ge 350$ GeV, $p_T^H < 200$ GeV	$0.9 \pm 0.7(\pm 0.6(stat.) \pm 0.3(syst.))$	0.88 ± 0.21
$gg \to H$, $200 \le p_T^H < 300$ GeV	$0.66^{+0.16}_{-0.15}(^{+0.13}_{-0.12}(stat.)^{+0.10}_{-0.08}(syst.))$	0.46 ± 0.10
$gg \to H$, $300 \le p_T^H < 450$ GeV	$0.08 \pm 0.05(^{+0.05}_{-0.04}(stat.) \pm 0.02(syst.))$	0.106 ± 0.027
$gg \to H$, $p_T^H \ge 450$ GeV	$0.036^{+0.024}_{-0.020}(^{+0.023}_{-0.020}(stat.)^{+0.008}_{-0.005}(syst.))$	0.018 ± 0.005
$qq \to Hqq$, $\le$ 1-jet	$0.6^{+2.0}_{-1.8}(^{+1.9}_{-1.8}(stat.) \pm 0.6(syst.))$	2.16 ± 0.06
$qq \to Hqq$, $\ge$ 2-jet, $m_{jj} < 350$ GeV, VH-enriched	$0.34^{+0.26}_{-0.24}(^{+0.23}_{-0.22}(stat.)^{+0.12}_{-0.11}(syst.))$	0.510 ± 0.016
$qq \to Hqq$, $\ge$ 2-jet, $m_{jj} < 350$ GeV, VBF-enriched	$1.8^{+1.1}_{-1.0}(^{+1.0}_{-0.9}(stat.)^{+0.5}_{-0.4}(syst.))$	0.735 ± 0.019
$qq \to Hqq$, $\ge$ 2-jet, $350 \le m_{jj} < 700$ GeV, $p_T^H < 200$ GeV	$0.49^{+0.26}_{-0.24}(^{+0.23}_{-0.21}(stat.)^{+0.13}_{-0.10}(syst.))$	0.535 ± 0.013
$qq \to Hqq$, $\ge$ 2-jet, $700 \le m_{jj} < 1000$ GeV, $p_T^H < 200$ GeV	$0.30^{+0.14}_{-0.12}(^{+0.12}_{-0.11}(stat.)^{+0.06}_{-0.05}(syst.))$	0.256 ± 0.007
$qq \to Hqq$, $\ge$ 2-jet, $1000 \le m_{jj} < 1500$ GeV, $p_T^H < 200$ GeV	$0.30^{+0.11}_{-0.10}(^{+0.10}_{-0.09}(stat.)^{+0.05}_{-0.04}(syst.))$	0.224 ± 0.006
$qq \to Hqq$, $\ge$ 2-jet, $m_{jj} \ge 1500$ GeV, $p_T^H < 200$ GeV	$0.26^{+0.08}_{-0.07}(\pm 0.07(stat.)^{+0.04}_{-0.03}(syst.))$	0.216 ± 0.006
$qq \to Hqq$, $\ge$ 2-jet, $350 \le m_{jj} < 1000$ GeV, $p_T^H \ge 200$ GeV	$0.04 \pm 0.05(^{+0.05}_{-0.04}(stat.)^{+0.02}_{-0.01}(syst.))$	0.0737 ± 0.0017
$qq \to Hqq$, $\ge$ 2-jet, $m_{jj} \ge 1000$ GeV, $p_T^H \ge 200$ GeV	$0.086^{+0.022}_{-0.021}(\pm 0.019(stat.)^{+0.011}_{-0.009}(syst.))$	0.0732 ± 0.0019
$qq \to Hl\nu$, $p_T^V < 75$ GeV	$0.70^{+0.30}_{-0.27}(^{+0.29}_{-0.26}(stat.)^{+0.06}_{-0.04}(syst.))$	0.215 ± 0.008
$qq \to Hl\nu$, $75 \le p_T^V < 150$ GeV	$0.05^{+0.11}_{-0.08}(^{+0.11}_{-0.08}(stat.)^{+0.02}_{-0.01}(syst.))$	0.134 ± 0.005
$qq \to Hl\nu$, $150 \le p_T^V < 250$ GeV	$0.039^{+0.019}_{-0.018}(\pm 0.013(stat.)^{+0.013}_{-0.012}(syst.))$	0.0412 ± 0.0017
$qq \to Hl\nu$, $250 \le p_T^V < 400$ GeV	$0.011 \pm 0.004(^{+0.004}_{-0.003}(stat.) \pm 0.002(syst.))$	0.0100 ± 0.0004
$qq \to Hl\nu$, $p_T^V \ge 400$ GeV	$0.0033^{+0.0020}_{-0.0018}(^{+0.0017}_{-0.0016}(stat.)^{+0.0011}_{-0.0009}(syst.))$	0.00214 ± 0.00011
$gg/qq \to Hll$, $p_T^V < 150$ GeV	$0.08 \pm 0.11(^{+0.09}_{-0.08}(stat.)^{+0.08}_{-0.07}(syst.))$	0.198 ± 0.007
$gg/qq \to Hll$, $150 \le p_T^V < 250$ GeV	$0.035^{+0.011}_{-0.010}(^{+0.009}_{-0.008}(stat.)^{+0.007}_{-0.006}(syst.))$	0.032 ± 0.004
$gg/qq \to Hll$, $250 \le p_T^V < 400$ GeV	$0.0074^{+0.0029}_{-0.0027}(^{+0.0025}_{-0.0024}(stat.)^{+0.0013}_{-0.0012}(syst.))$	0.0072 ± 0.0008
$gg/qq \to Hll$, $p_T^V \ge 400$ GeV	$0.0004^{+0.0012}_{-0.0011}(^{+0.0010}_{-0.0009}(stat.)^{+0.0007}_{-0.0006}(syst.))$	0.00126 ± 0.00010
$t\bar{t}H$, $p_T^H < 60$ GeV	$0.09^{+0.09}_{-0.08}(^{+0.08}_{-0.07}(stat.)^{+0.04}_{-0.03}(syst.))$	0.118 ± 0.016
$t\bar{t}H$, $60 \le p_T^H < 120$ GeV	$0.13^{+0.10}_{-0.09}(^{+0.09}_{-0.08}(stat.)^{+0.05}_{-0.04}(syst.))$	0.178 ± 0.020
$t\bar{t}H$, $120 \le p_T^H < 200$ GeV	$0.05 \pm 0.06(\pm 0.05(stat.) \pm 0.03(syst.))$	0.126 ± 0.015
$t\bar{t}H$, $200 \le p_T^H < 300$ GeV	$0.052^{+0.030}_{-0.027}(^{+0.026}_{-0.024}(stat.)^{+0.015}_{-0.012}(syst.))$	0.053 ± 0.007
$t\bar{t}H$, $300 \le p_T^H < 450$ GeV	$0.005^{+0.012}_{-0.011}(\pm 0.010(stat.) \pm 0.006(syst.))$	0.0190 ± 0.0031
$t\bar{t}H$, $p_T^H \ge 450$ GeV	$0.000 \pm 0.008(^{+0.006}_{-0.005}(stat.) \pm 0.005(syst.))$	0.0054 ± 0.0010
tH	$0.5^{+0.4}_{-0.3}(\pm 0.3(stat.)^{+0.2}_{-0.1}(syst.))$	$0.085^{+0.005}_{-0.011}$

Best-fit values and uncertainties for the cross sections in each measurement region

Higgs boson mass in $H \to \gamma\gamma$ and $H \to ZZ^* \to 4\ell$ arXiv:2308.04775

Source	Systematic uncertainty on m_H [MeV]
e/γ E_{T}-independent $Z \to ee$ calibration	44
e/γ E_{T}-dependent electron energy scale	28
$H \to \gamma\gamma$ interference bias	17
e/γ photon lateral shower shape	16
e/γ photon conversion reconstruction	15
e/γ energy resolution	11
$H \to \gamma\gamma$ background modelling	10
Muon momentum scale	8
All other systematic uncertainties	7

x-sections in ggF $H \to WW^* \to e\nu\mu\nu$ EPJC 83 (2023) 774

Process	Matrix element (alternative)	PDF set	UE and PS model (alternative model)	Prediction order for total cross section
ggF H	POWHEG BOX v2 [18,19,20,21,22] NNLOPS [66,18,25] (MG5_AMC@NLO) [42,67]	PDF4LHC15NNLO [54]	PYTHIA 8 [65] (HERWIG 7) [68]	N^3LO QCD + NLO EW [31,32,33,34,35,36,37,38,39,40,41]
VBF H	POWHEG BOX v2 [66,20,21,22] (MG5_AMC@NLO)	PDF4LHC15NLO	PYTHIA 8 (HERWIG 7)	NNLO QCD + NLO EW [44,45,46]
VH excl. $gg \to ZH$	POWHEG BOX v2	PDF4LHC15NLO	PYTHIA 8	NNLO QCD + NLO EW [47,48,49,51,52]
ttH	POWHEG BOX v2	NNPDF3.0NLO	PYTHIA 8	NLO [31]
$gg \to ZH$	POWHEG BOX v2	NNPDF3.0NLO	PYTHIA 8	NLO+NLL [50,53]
$qq \to WW$	SHERPA 2.2.2 [69] (Q_{cut})	NNPDF3.0NNLO [70]	SHERPA 2.2.2 [71,72,73,74,75,76] (SHERPA 2.2.2 [72,80]; μ_q)	NLO [77,78,79]
$qq \to WWqq$	MG5_AMC@NLO [42]	NNPDF3.0NLO	PYTHIA 8 (HERWIG 7)	LO
$gg \to WW/ZZ$	SHERPA 2.2.2	NNPDF3.0NNLO	SHERPA 2.2.2	LO [81]
$WZ/V\gamma^*/ZZ$	SHERPA 2.2.2	NNPDF3.0NNLO	SHERPA 2.2.2	NLO [82]
$V\gamma$	SHERPA 2.2.8 [69]	NNPDF3.0NNLO	SHERPA 2.2.8	NLO [82]
VVV	SHERPA 2.2.2	NNPDF3.0NNLO	SHERPA 2.2.2	NLO
$t\bar{t}$	POWHEG BOX v2 (MG5_AMC@NLO)	NNPDF3.0NLO	PYTHIA 8 (HERWIG 7)	NNLO+NNLL [83,84,85,86,87,88,89]
Wt	POWHEG BOX v2 (MG5_AMC@NLO)	NNPDF3.0NLO	PYTHIA 8 (HERWIG 7)	NNLO [90,91]
Z/γ^*	SHERPA 2.2.1 (MG5_AMC@NLO)	NNPDF3.0NNLO	SHERPA 2.2.1	NNLO [92]

x-sections in ggF $H \to WW^* \to e\nu\mu\nu$ EPJC 83 (2023) 774

Category	$N_{\text{jet},(p_T>30\ \text{GeV})} = 0$	$N_{\text{jet},(p_T>30\ \text{GeV})} = 1$
Pre-Selection	Exactly two isolated leptons ($\ell = e, \mu$) with opposite charge $p_T^{\text{lead}} > 22\,GeV$, $p_T^{\text{sublead}} > 15\,GeV$ $\lvert\eta_e\rvert < 2.5$, $\lvert\eta_\mu\rvert < 2.5$, $p_T^{\text{jet}} > 30\,GeV$ $m_{\ell\ell} > 10\,GeV$ $E_T^{\text{miss, track}} > 20\,GeV$	
Background rejection	$N_{b\text{-jet},(p_T>20\,\text{GeV})} = 0$ $\Delta\phi_{\ell\ell,E_T^{\text{miss}}} > \pi/2$ $p_T^{\ell\ell} > 30\,GeV$	$N_{b\text{-jet},(p_T>20\,\text{GeV})} = 0$ $\max(m_T^{\ell}) > 50\,GeV$ $m_{\tau\tau} < m_Z - 25\,GeV$ $m_T > 80\,GeV$
$H \to WW^* \to \ell\nu\ell\nu$ topology	$m_{\ell\ell} < 55\,GeV$ $\Delta\phi_{\ell\ell} < 1.8$	

Event selection criteria used to define the signal and fiducial region in the analysis. The reconstructed electrons are required to have a pseudorapidity $|\eta| < 2.47$, excluding the transition region between the barrel and endcaps of the EM calorimeter, $1.37 < |\eta| < 1.52$.

x-sections in ggF $H \to WW^* \to e\nu\mu\nu$ EPJC 83 (2023) 774

<table>
<tr><th>CR</th><th>$N_{\text{jet},(p_T>30\text{ GeV})} = 0$</th><th>$N_{\text{jet},(p_T>30\text{ GeV})} = 1$</th></tr>
<tr><td rowspan="2">$qq \to WW$</td><td colspan="2">$N_{b\text{-jet},(p_T>20\text{ GeV})} = 0$</td></tr>
<tr><td>$\Delta\phi_{\ell\ell,E_T^{\text{miss}}} > \pi/2$
$p_T^{\ell\ell} > 30$ GeV
$\mathbf{55 < m_{\ell\ell} < 110}$ **GeV**
$\mathbf{\Delta\phi_{\ell\ell} < 2.6}$</td><td>$\mathbf{m_{\ell\ell} > 80}$ **GeV**
$\mathbf{|m_{\tau\tau} - m_Z| > 25}$ **GeV**
$\max\left(m_T^{\ell}\right) > 50$ GeV</td></tr>
<tr><td>$t\bar{t}/Wt$</td><td>$\mathbf{N_{b\text{-jet},(20\text{ GeV}<p_T<30\text{ GeV})} > 0}$
$\Delta\phi_{\ell\ell,E_T^{\text{miss}}} > \pi/2$
$p_T^{\ell\ell} > 30$ GeV
$\mathbf{\Delta\phi_{\ell\ell} < 2.8}$</td><td>$\mathbf{N_{b\text{-jet},(p_T>30\text{ GeV})} = 1}$
$N_{b\text{-jet},(20\text{ GeV}<p_T<30\text{ GeV})} = 0$
$m_{\tau\tau} < m_Z - 25$ GeV
$\max\left(m_T^{\ell}\right) > 50$ GeV</td></tr>
<tr><td rowspan="2">$Z/\gamma^* \to \tau\tau$</td><td colspan="2">$N_{b\text{-jet},(p_T>20\text{ GeV})} = 0$
$\mathbf{m_{\ell\ell} < 80}$ **GeV**
no $\mathbf{E_T^{\text{miss, track}}}$ **requirement**</td></tr>
<tr><td>$\mathbf{\Delta\phi_{\ell\ell} > 2.8}$</td><td>$\mathbf{m_{\tau\tau} > m_Z - 25}$ **GeV**
$\max\left(m_T^{\ell}\right) > 50$ GeV</td></tr>
</table>

Background	Normalization factor
$qqWW$ $N_{\text{jet}} = 0$	0.97 ± 0.07
$qqWW$ $N_{\text{jet}} = 1$	0.91 ± 0.13
Z+jets $N_{\text{jet}} = 0$	0.91 ± 0.07
Z+jets $N_{\text{jet}} = 1$	1.02 ± 0.12
Top $N_{\text{jet}} = 0$	1.07 ± 0.24
Top $N_{\text{jet}} = 1$	1.03 ± 0.18

x-sections in ggF $H \to WW^* \to e\nu\mu\nu$ EPJC 83 (2023) 774

Variable	Data Statistical [%]	MC Statistical [%]	Experimental [%]	Theory [%]
$y_{\ell\ell}$	14–22	5.3–10	6.9–15	5.9–15
$p_{\mathrm{T}}^{\ell\ell}$	15–29	6.4–14	8.2–31	6.8–27
$p_{\mathrm{T}}^{\ell 0}$	13–28	6.3–13	9.3–28	14–34
$\Delta\phi_{\ell\ell}$	11–39	6.1–18	7.8–22	13–27
y_{j0}	23–51	12–26	21–54	26–58
$\cos\theta^*$	11–15	5.8–7.6	8.5–11	8.9–14
p_{T}^{H}	8.5–72	6.2–18	10–58	12–27
$m_{\ell\ell}$	12–25	5.6–11	7.5–15	7.3–20
$y_{\ell\ell}$ vs N_{jet}	9.0–62	3.9–25	8.0–20	5.0–53
$p_{\mathrm{T}}^{\ell\ell}$ vs N_{jet}	9.8–36	4.7–20	12–41	9.9–50
$p_{\mathrm{T}}^{\ell 0}$ vs N_{jet}	9.6–50	5.8–20	10–35	9.4–74
$\Delta\phi_{\ell\ell}$ vs N_{jet}	9.6–65	5.6–18	6.8–31	14–74
$\cos\theta^*$ vs N_{jet}	13–50	6.8–25	7.7–39	8.9–58
$m_{\ell\ell}$ vs N_{jet}	12–152	5.7–44	8.9–58	7.2–82

x-sections in VBF $H \rightarrow WW^{*} \rightarrow e\nu\mu\nu$ PRD 108, 072003

Simulation Name	Generator	ME Accuracy	PDF	Shower & Hadronization	UE & PS Parameter Set
Powheg+Pythia 8	POWHEG-BOX v2	NLO QCD & EW + approx. NNLO QCD	NNPDF3.0NLO	Pythia 8.230 +EvtGen v1.6.0	AZNLO
Powheg+Herwig 7	POWHEG-BOX v2	NLO QCD & EW + approx. NNLO QCD	NNPDF3.0NLO	Herwig 7.1.3 +EvtGen v1.6.0	H7UE
MG5+Herwig 7	MadGraph5_aMC@NLO	NLO QCD, LO EW	NNPDF30NLO	Herwig 7.1.6 EvtGen v1.7.0	H7UE
VBFNLO@LO	VBFNLO 2.7.1	LO QCD & EW	NNPDF3.0NLO CT14, MMHT14	-	-
VBFNLO@NLO	VBFNLO 2.7.1	NLO QCD & EW	NNPDF3.0NLO CT14, MMHT14	-	-
VBFNLO@LO+Pythia 8	VBFNLO 2.7.1	LO QCD & EW	NNPDF3.0NLO CT14, MMHT14	Pythia 8.244 +EvtGen v1.7.0	A14

Summary of generators used for simulating the signal VBF $H \rightarrow WW^{*} \rightarrow e\nu\mu\nu$ processes

x-sections in VBF $H \to WW^* \to e\nu\mu\nu$ PRD 108, 072003

Selection Requirements	Signal Region	Fiducial Region
Lepton pair flavors	e-μ	
Lepton pair charge	0	
Leading (subleading) lepton p_{T}	> 22 GeV (> 15 GeV)	
Lepton η^{ℓ}	$\|\eta^{\mu}\| < 2.5$ $0 < \|\eta^{e}\| < 1.37$ or $1.52 < \|\eta^{e}\| < 2.47$	$\|\eta^{\mu}\| < 2.5$ $\|\eta^{e}\| < 2.5$
No. of additional leptons	0	
$\Delta R(\ell, \ell)$	overlap removal	> 0.1
$m_{\ell\ell}$	> 10 GeV	
$\Delta R(\ell, \mathrm{jet})$	overlap removal	> 0.4
No. of jets ($p_{\mathrm{T}} > 30$ GeV, $\|\eta\| < 4.5$)	≥ 2	
No. of b-jets ($p_{\mathrm{T}} > 20$ GeV, $\|\eta\| < 2.5$)	0	
$m_{\tau\tau}$	$< m_Z - 25$ GeV	
Central jet veto ($p_{\mathrm{T}} > 20$ GeV)	✓	
Outside lepton veto	✓	
m_{jj}	> 450 GeV	
$\|\Delta y_{jj}\|$	> 2.1	
$\|\Delta \phi_{\ell\ell}\|$	< 1.4 rad	

x-sections in VBF $H \to WW^* \to e\nu\mu\nu$

PRD 108, 072003

Sample	SR	Z/γ^*+jets CR	ggF CR
Signal (POWHEG+PYTHIA 8)	110	13	86
ggF Higgs	39	4	450
Other Higgs	3	10	78
Top	420	41	11 000
Z/γ^*+jets	79	320	1 400
VV	280	32	4 300
$V\gamma$	13	14	210
Mis-Id	47	12	810
Total Signal+Background	1 000 ± 120	450 ± 160	18 800 ± 2 600
Data	916	406	18 228

x-sections in VBF $H \to WW^* \to e\nu\mu\nu$

PRD 108, 072003

Source	Uncertainty [%] σ^{fid}	Uncertainty range [%] p_T^H	$p_T^{\ell\ell}$, $p_T^{\ell_1}$, $p_T^{\ell_2}$, $\lvert\Delta y_{\ell\ell}\rvert$, $\lvert\Delta\phi_{\ell\ell}\rvert$, $\cos(\theta_\eta^*)$	$m_{\ell\ell}$	$p_T^{j_1}$, $p_T^{j_2}$, $\lvert\Delta y_{jj}\rvert$, $\Delta\phi_{jj}$	m_{jj}
Signal modeling	5	< 1 – 7	< 1 – 7	< 1 – 19	< 1 – 8	2 – 7
Signal parton shower	< 1	< 1 – 2	< 1 – 1.8	< 1 – 10	< 1 – 1.8	< 1 – 7
$t\bar{t}$ modeling	6	1.7 – 30	3 – 13	3 – 80	3 – 10	1.2 – 70
WW modeling	4	< 1 – 12	3 – 11	2 – 90	3 – 10	3 – 40
Z/γ^*+jets modeling	4	< 1 – 19	2 – 18	4 – 30	3 – 13	2 – 50
ggF modeling	5	4.0 – 28	3.4 – 10	2.6 – 12	2.3 – 9.0	1.4 – 86
Mis-Id background	< 1	< 1 – 12	1.1 – 5	< 1 – 19	1 – 3	< 1 – 40
Jets & Pile-up & E_T^{miss}	5	8 – 60	6 – 30	6 – 120	9 – 30	9 – 130
b-tagging	< 1	< 1 – 9	< 1 – 3	< 1 – 19	1.1 – 3	< 1 – 40
Leptons	1.5	3 – 17	2 – 9	1.2 – 13	1.7 – 7	< 1 – 16
Luminosity	1.5	1.7 – 2	1.3 – 1.9	< 1 – 4	1.5 – 2	< 1 – 1.9
MC statistics	5	10 – 40	6 – 30	6 – 180	8 – 30	7 – 90
Total systematics	13	19 – 90	13 – 60	12 – 180	15 – 50	15 – 200
Data statistics	20	50 – 160	30 – 110	30 – 400	40 – 100	50 – 300
Total uncertainty	23	50 – 190	40 – 120	30 – 500	40 – 100	50 – 400

x-sections in VBF $H \to WW^* \to e\nu\mu\nu$

PRD 108, 072003

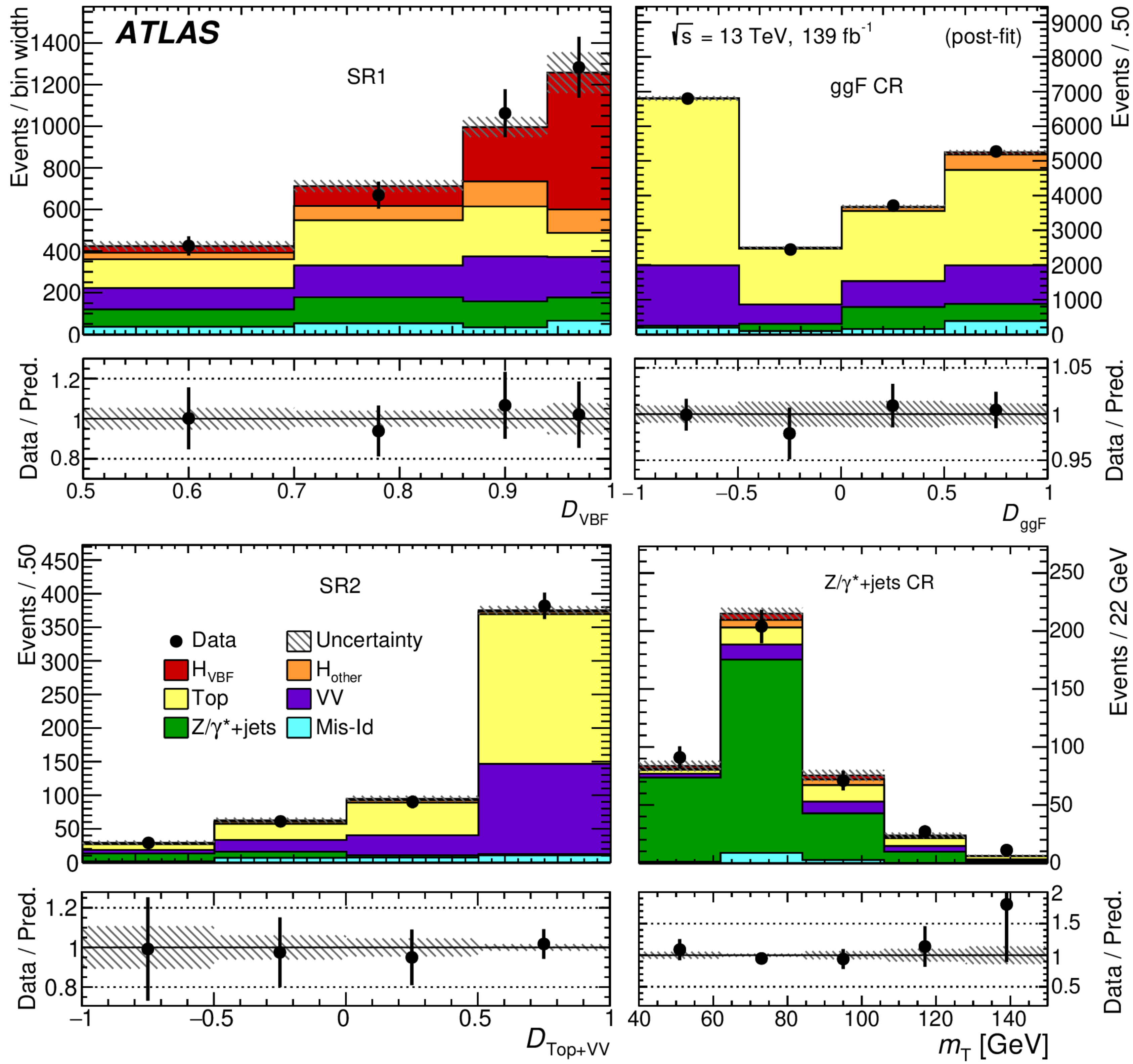

Higgs boson mass

PLB 847 (2023) 138315

Category	$\sigma_{90}^{\gamma\gamma}$ [GeV]	S_{90}	B_{90}	f_{90} [%]	Z_{90}
U, Central-barrel, high $p_{\mathrm{Tt}}^{\gamma\gamma}$	1.88	42	65	39.1	4.7
U, Central-barrel, medium $p_{\mathrm{Tt}}^{\gamma\gamma}$	2.34	102	559	15.4	4.2
U, Central-barrel, low $p_{\mathrm{Tt}}^{\gamma\gamma}$	2.63	837	13 226	6.0	7.2
U, Outer-barrel, high $p_{\mathrm{Tt}}^{\gamma\gamma}$	2.16	31	83	27.4	3.3
U, Outer-barrel, medium $p_{\mathrm{Tt}}^{\gamma\gamma}$	2.63	108	981	9.9	3.4
U, Outer-barrel, low $p_{\mathrm{Tt}}^{\gamma\gamma}$	3.00	869	22 919	3.7	5.7
U, Endcap	3.33	759	29 383	2.5	4.4
C, Central-barrel, high $p_{\mathrm{Tt}}^{\gamma\gamma}$	2.10	26	44	37.3	3.6
C, Central-barrel, medium $p_{\mathrm{Tt}}^{\gamma\gamma}$	2.62	62	389	13.8	3.1
C, Central-barrel, low $p_{\mathrm{Tt}}^{\gamma\gamma}$	3.00	508	9 726	5.0	5.1
C, Outer-barrel, high $p_{\mathrm{Tt}}^{\gamma\gamma}$	2.56	34	103	25.0	3.2
C, Outer-barrel, medium $p_{\mathrm{Tt}}^{\gamma\gamma}$	3.20	114	1 353	7.8	3.1
C, Outer-barrel, low $p_{\mathrm{Tt}}^{\gamma\gamma}$	3.71	914	30 121	2.9	5.2
C, Endcap	4.04	1 249	52 160	2.3	5.5
Inclusive	3.32	5 653	128 774	4.2	15.6

Higgs boson mass

PLB 847 (2023) 138315

Source	Impact [MeV]
Photon energy scale	83
$Z \to e^+e^-$ calibration	59
E_{T}-dependent electron energy scale	44
$e^{\pm} \to \gamma$ extrapolation	30
Conversion modelling	24
Signal–background interference	26
Resolution	15
Background model	14
Selection of the diphoton production vertex	5
Signal model	1
Total	90

Higgs boson width in $H^* \to ZZ \to 4\ell/2\ell 2\nu$ PLB 846 (2023) 138223

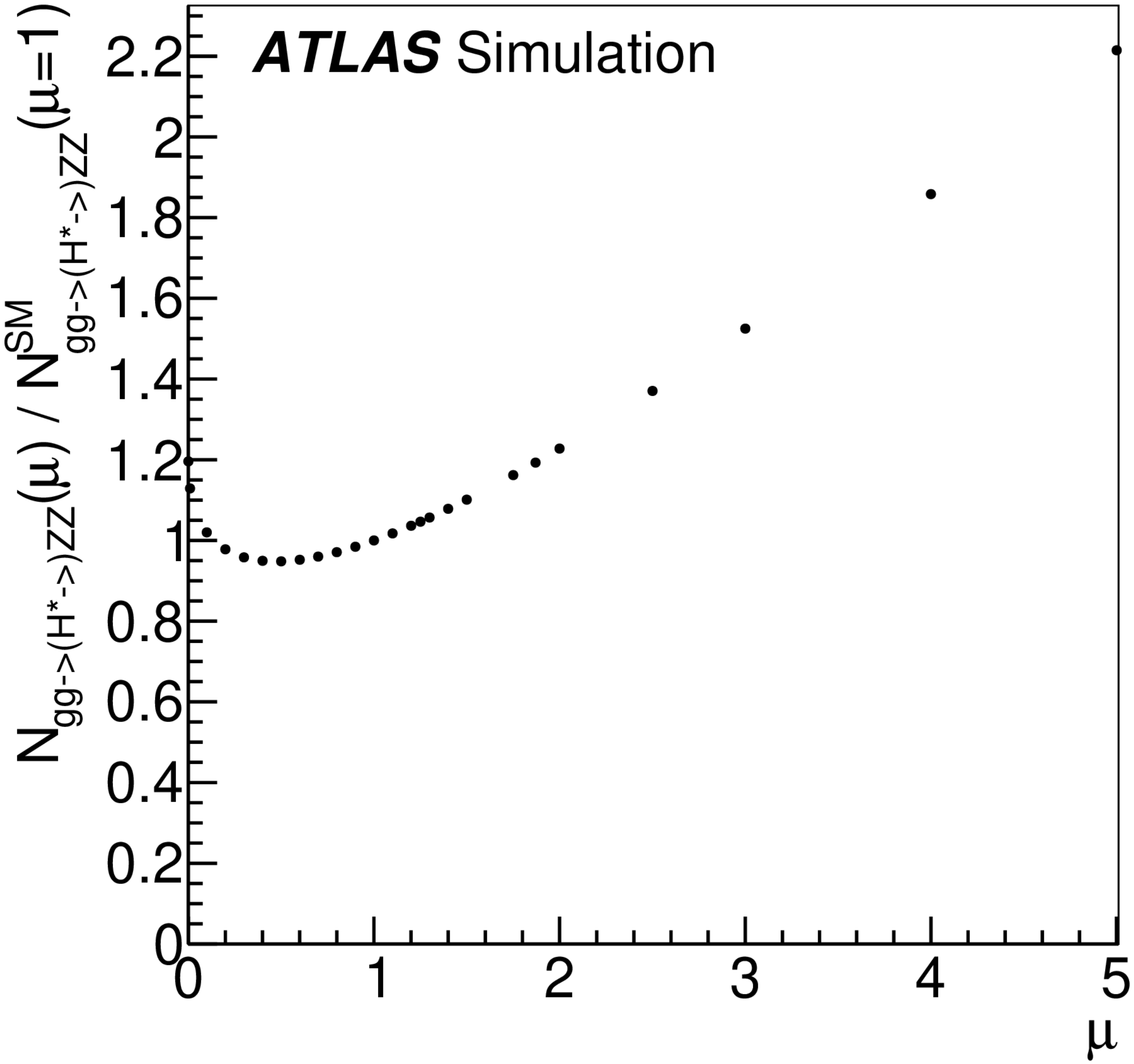

Parabolic dependence of the yield of the $gg \to (H^* \to)ZZ$ process on $\mu_{\text{off-shell}}$.

Higgs boson width in $H^* \to ZZ \to 4\ell/2\ell2\nu$ PLB 846 (2023) 138223

4ℓ

Process	ggF SR	Mixed SR	EW SR
$gg \to (H^* \to)ZZ$	341 ± 117	42.5 ± 14.9	11.8 ± 4.3
$gg \to H^* \to ZZ$	32.6 ± 9.07	3.68 ± 1.03	1.58 ± 0.47
$gg \to ZZ$	345 ± 119	43.0 ± 15.2	11.9 ± 4.4
$qq \to (H^* \to)ZZ + 2j$	23.2 ± 1.0	2.03 ± 0.16	9.89 ± 0.96
$qq \to ZZ$	1878 ± 151	135 ± 23	22.0 ± 8.3
Other backgrounds	50.6 ± 2.5	1.79 ± 0.16	1.65 ± 0.16
Total expected (SM)	2293 ± 209	181 ± 29	45.3 ± 10.0
Observed	2327	178	50

$2\ell2\nu$

Process	ggF SR	Mixed SR	EW SR
$gg \to (H^* \to)ZZ$	210 ± 53	19.7 ± 4.9	4.29 ± 1.10
$gg \to H^* \to ZZ$	111 ± 26	10.9 ± 2.5	3.26 ± 0.82
$gg \to ZZ$	251 ± 66	23.4 ± 6.2	5.31 ± 1.46
$qq \to (H^* \to)ZZ + 2j$	14.0 ± 3.0	1.63 ± 0.17	4.46 ± 0.50
$qq \to ZZ$	1422 ± 112	80.4 ± 11.9	7.74 ± 2.99
WZ	678 ± 54	51.9 ± 6.9	7.89 ± 2.50
Z+jets	62.3 ± 24.3	7.51 ± 6.94	0.62 ± 0.54
Non-resonant-$\ell\ell$	106 ± 39	9.17 ± 2.73	1.55 ± 0.42
Other backgrounds	22.6 ± 5.2	1.62 ± 0.25	1.40 ± 0.10
Total expected (SM)	2515 ± 165	172 ± 17	28.0 ± 4.1
Observed	2496	181	27

Higgs boson width in $H^* \to ZZ \to 4\ell/2\ell 2\nu$ PLB 846 (2023) 138223

Process	Uncertainty	Final State	Value (%)
ggF Signal Region			
$qq \to ZZ$	QCD Scale	$2\ell 2\nu$	4–40
$qq \to ZZ + 2j$	QCD Scale	4ℓ	21–28
$qq \to ZZ + 2j$	QCD Scale	$2\ell 2\nu$	22–37
$qq \to ZZ + 2j$	Parton Shower	$2\ell 2\nu$	1–67
$gg \to H^* \to ZZ$	Parton Shower	4ℓ	27
$gg \to H^* \to ZZ$	Parton Shower	$2\ell 2\nu$	8–45
$gg \to ZZ$	Parton Shower	4ℓ	38
$gg \to ZZ$	Parton Shower	$2\ell 2\nu$	6–43
$WZ + 0j$	QCD Scale	$2\ell 2\nu$	1–54
1-jet Signal Region			
$gg \to H^* \to ZZ$	Parton Shower	4ℓ	27
$gg \to H^* \to ZZ$	QCD Scale	$2\ell 2\nu$	13–18
$gg \to ZZ$	Parton Shower	4ℓ	38
$gg \to ZZ$	QCD Scale	$2\ell 2\nu$	18–20
$qq \to ZZ$ (EW)	QCD Scale	$2\ell 2\nu$	7–18
2-jet Signal Region			
$qq \to ZZ + 2j$	QCD Scale	4ℓ	18–26
$qq \to ZZ + 2j$	QCD Scale	$2\ell 2\nu$	8–32
$gg \to H^* \to ZZ$	Parton Shower	4ℓ	27
$gg \to ZZ$	Parton Shower	4ℓ	38
$gg \to ZZ$	QCD Scale	$2\ell 2\nu$	18–20
$WZ + 2j$	QCD Scale	$2\ell 2\nu$	20–22
$qq \to ZZ$ Control Regions			
$qq \to ZZ + 2j$	QCD Scale	4ℓ	26
Three-lepton Control Regions			
$WZ + 2j$	QCD Scale	$2\ell 2\nu$	28

Higgs boson width in $H^* \to ZZ \to 4\ell/2\ell 2\nu$ PLB 846 (2023) 138223

Systematic Uncertainty Fixed	$\mu_{\text{off-shell}}$ value at which $-2\ln\lambda(\mu_{\text{off-shell}}) = 4$
Parton shower uncertainty for $gg \to ZZ$ (normalisation)	2.26
Parton shower uncertainty for $gg \to ZZ$ (shape)	2.29
NLO EW uncertainty for $qq \to ZZ$	2.27
NLO QCD uncertainty for $gg \to ZZ$	2.29
Parton shower uncertainty for $qq \to ZZ$ (shape)	2.29
Jet energy scale and resolution uncertainty	2.26
None	2.30

The impact of most important systematic uncertainties on the observed upper value of $\mu_{\text{off-shell}}$ for which $-2\ln\lambda = 4$, obtained by the combined fit.

Challenges of the off-shell Higgs regime

The signal $gg \to H^* \to VV$ process proceeds predominantly through a **top-quark loop**.

- **On-shell**: top-quark mass is the largest scale in the process and can be **approximated as infinitely heavy** ⇒ loop-induced process can be reduced to a tree-level one.
- **Off-shell**: virtuality of the Higgs boson may be comparable to (or larger than) the top-quark mass ⇒ the **impact of top quarks** in the loops cannot be neglected.
  - LO prediction requires the computation of a one-loop amplitude with the full top mass dependence, while the NLO correction requires a two-loop amplitude calculation.
  - Contribution from both massless and massive quarks circulating in the loops should be considered in the background $gg \to VV$ amplitude computation.
  - Sizeable destructive interference effects between the signal and the background process ⇒must be taken into account.

Off-shell Higgs: 4ℓ final state strategy

PLB 846 (2023) 138223

- Final state decay objects (e and μ) can be fully reconstructed.
- **Signal regions** defined as $m_{4\ell} > 220$ GeV, designed to target the **EW** (VBF+VH) and **ggF** productions.
  - **EW SR** ($n_{\text{jets}} \geq 2$ and $|\Delta\eta_{jj}| > 4.0$) and **Mixed SR** ($n_{\text{jets}} = 1$ and $\eta_j > 2.2$)
  - **ggF SR**: remaining events
- **Observables**: NN methods trained with kinematic variables and ME discriminants sensitive to the signal.

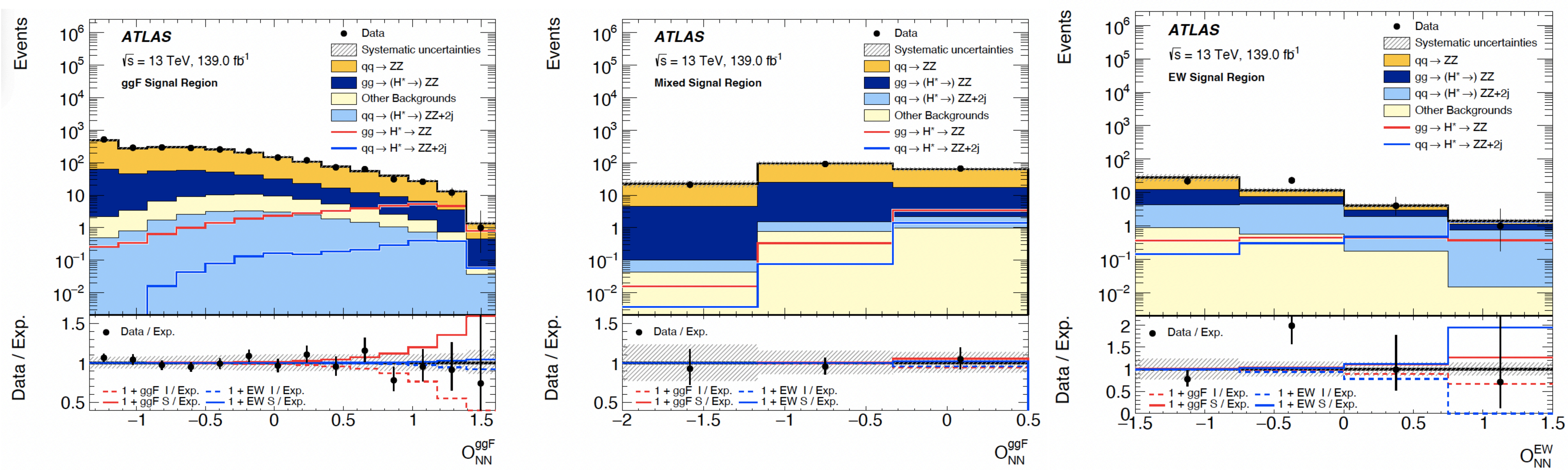

Off-shell Higgs: 4ℓ final state strategy

PLB 846 (2023) 138223

- Final state decay objects (e and μ) can be fully reconstructed.
- **Signal regions** defined as $m_{4\ell} > 220$ GeV, designed to target the **EW** (VBF+VH) and **ggF** productions.
  - **EW SR** ($n_{\text{jets}} \geq 2$ and $|\Delta\eta_{jj}| > 4.0$) and **Mixed SR** ($n_{\text{jets}} = 1$ and $\eta_j > 2.2$)
  - **ggF SR**: remaining events
- **Observables**: NN methods trained with kinematic variables and ME discriminants sensitive to the signal.

4ℓ final state full kinematics → dense NN → $O_{\text{NN}}^{\text{ggF}}{}^{*} = \log \dfrac{P_S^{\text{ggF}}}{P_B^{\text{ggF}} + P_{q\bar{q}ZZ}}$

$4\ell + 2j$ final state full kinematics → dense NN → $O_{\text{NN}}^{\text{EW}} = \log \dfrac{P_S^{\text{EW}}}{P_B^{\text{EW}} + P_{q\bar{q}ZZ}}$

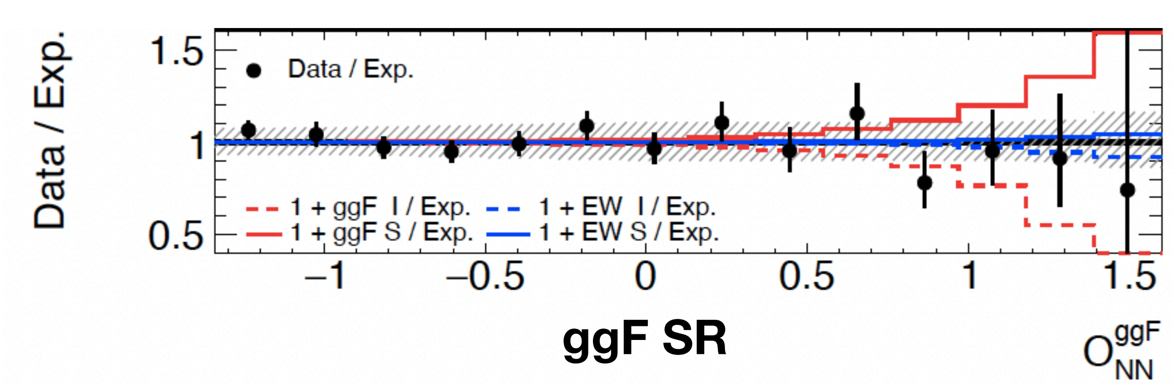

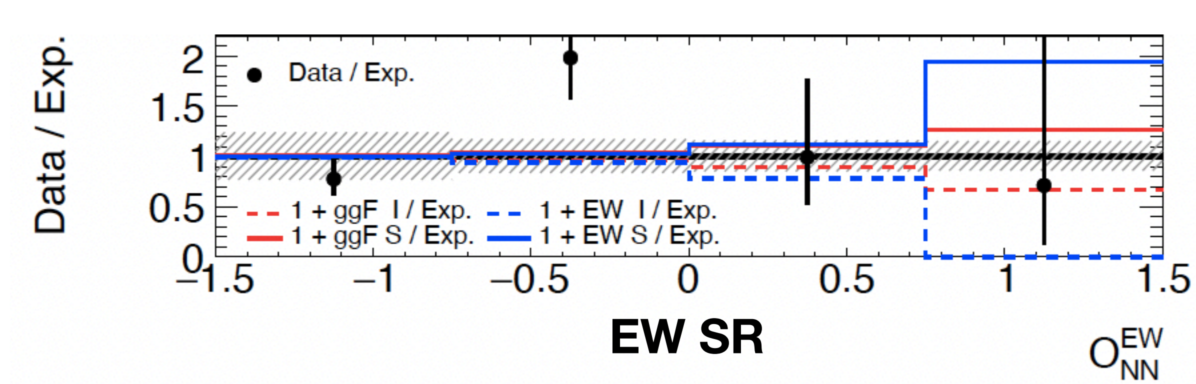

⇒ Good job of enhancing S/Exp. at higher values

*Also used for Mixed SR

Off-shell Higgs: $2\ell 2\nu$ final state strategy **PLB 846 (2023) 138223**

- Six times larger branching ratio (compared to the 4ℓ final state).
- **Signal regions** defined as $m_{4\ell} > 220$ GeV, designed to target the **EW** (VBF+VH) and **ggF** productions.
  - **EW SR** ($n_{\text{jets}} \geq 2$ and $|\Delta\eta_{jj}| > 4.0$) and **Mixed SR** ($n_{\text{jets}} = 1$ and $\eta_j > 2.2$)
  - **ggF SR**: remaining events
- **Observables**: NN methods trained with kinematic variables and ME discriminants sensitive to the signal.

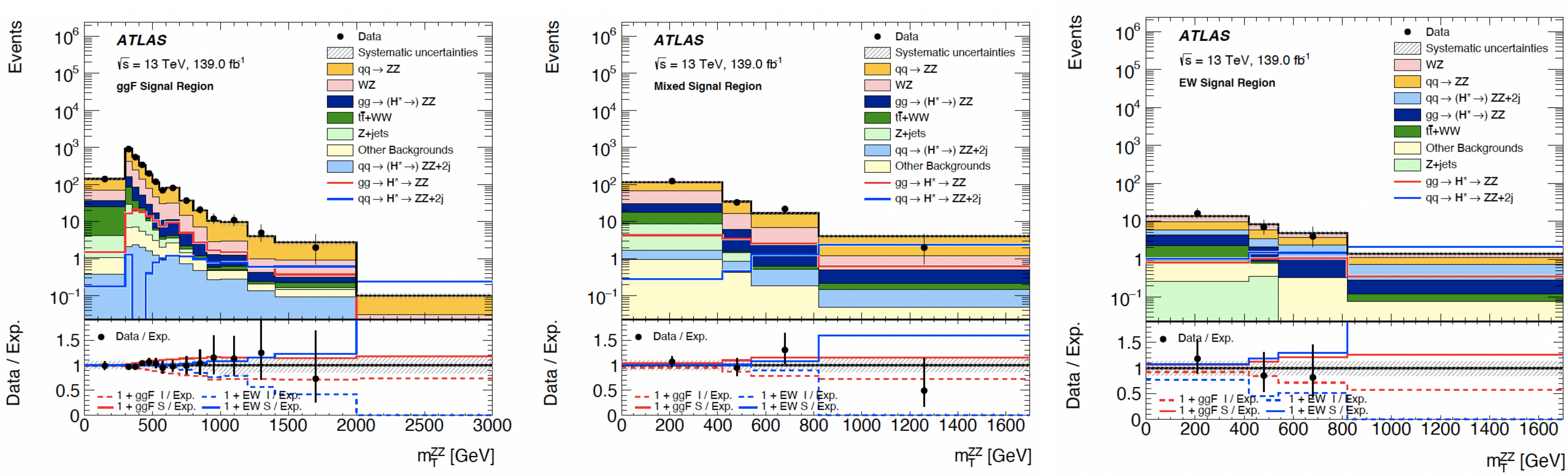

Off-shell Higgs: $2\ell 2\nu$ final state strategy PLB 846 (2023) 138223

- Six times larger branching ratio (compared to the 4ℓ final state).
- **Signal regions** defined as $m_{4\ell} > 220$ GeV, designed to target the **EW** (VBF+VH) and **ggF** productions.
  - **EW SR** ($n_{\text{jets}} \geq 2$ and $|\Delta\eta_{jj}| > 4.0$) and **Mixed SR** ($n_{\text{jets}} = 1$ and $\eta_j > 2.2$)
  - **ggF SR**: remaining events
- **Observables**: transverse mass of the ZZ system (m_{T}^{ZZ})

$$m_{\mathrm{T}}^{ZZ} \equiv \sqrt{\left[\sqrt{m_Z^2 + \left(p_{\mathrm{T}}^{\ell\ell}\right)^2} + \sqrt{m_Z^2 + \left(E_{\mathrm{T}}^{\text{miss}}\right)^2}\right]^2 - \left|\vec{p}_{\mathrm{T}}^{\,\ell\ell} + \vec{E}_{\mathrm{T}}^{\text{miss}}\right|^2}$$

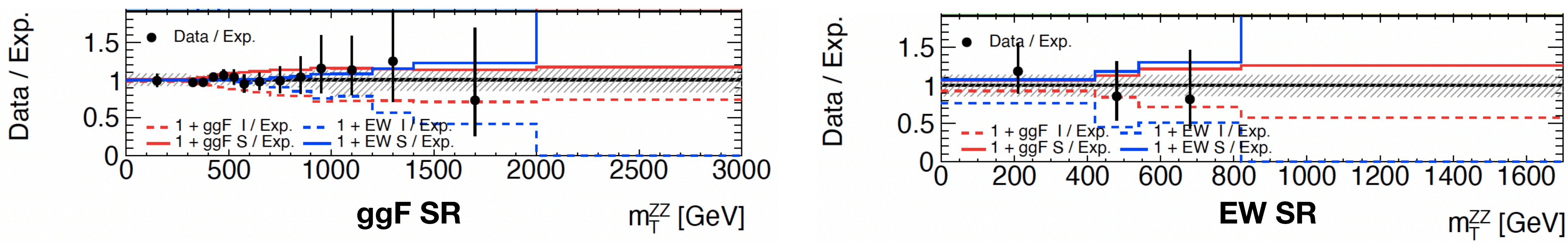

⇒ Good job of enhancing S/Exp.

Off-shell Higgs: MC modelling and bkg normalization PLB 846 (2023) 138223

Signal and background modelling

- $gg \to (H^* \to)ZZ$: Sherpa 2.2.2 + 0,1j@LO + QCD NLO/LO K-factors + N3LO/NLO flat K-factor of 1.32
- $qq \to (H^* \to)ZZ + 2\mathrm{j}$: MadGraph5 @LO
- $q\bar{q} \to ZZ$: Sherpa 2.2.2 + 0,1j@NLO +2,3j@LO + EW NLO corrections for 4l, 2l2v
- WZ: Sherpa 2.2.1 + 0,1j@NLO +2,3j@LO

Normalizations of the main background sources determined by data

- Dedicated **control regions** introduced to constrain each of the data-driven normalization factors.
- 4ℓ and $2\ell 2\nu$ channels: $qqZZ$ (dominant background in all SRs)
  - Constrained using three 4ℓ CRs: $180 < m_{4\ell} < 220$ GeV, $N_{\mathrm{jet}} = 0/1/\geq 2$
- $2\ell 2\nu$ channel: WZ, $Z + \mathrm{jets}$ and non-resonant $\ell\ell$ production (mostly $t\bar{t}$ and WW)